FACULDADE DE BIOCIÊNCIAS
PROGRAMA DE PÓS-GRADUAÇÃO EM BIOLOGIA CELULAR E MOLECULAR
MESTRADO EM BIOLOGIA CELULAR E MOLECULAR

LUIZA GALINA

CARACTERIZAÇÃO BIOQUÍMICA DA ENZIMA ADENILOSUCCINATO LIASE DE *LEISHMANIA* (*VIANNIA*) *BRAZILIENSIS* VISANDO O PLANEJAMENTO RACIONAL DE FÁRMACOS ANTILEISHMANIOSES

Porto Alegre

2017

Pontifícia Universidade Católica do Rio Grande do Sul

Faculdade de Biociências

Programa de Pós-Graduação em Biologia Celular e Molecular

Luiza Galina

Caracterização bioquímica da enzima Adenilosuccinato liase de *Leishmania* (*Viannia*) *braziliensis* visando o planejamento racional de fármacos antileishmanioses

Porto Alegre
2017

Luiza Galina

Caracterização bioquímica da enzima adenilosuccinato liase de *Leishmania* (*Viannia*) *braziliensis* visando o planejamento racional de fármacos antileishmanioses

Dissertação apresentada ao Programa de Pós-Graduação em Biologia Celular e Molecular da Faculdade de Biologia da Pontifícia Universidade Católica do Rio Grande do Sul.

Orientador: Prof. Dr. Luiz Augusto Basso

Porto Alegre
2017

Ficha Catalográfica

G158 Galina, Luiza

Caracterização bioquímica da enzima adenilosuccinato liase de Leishmania (Viannia) braziliensis visando o planejamento racional de fármacos antileishmanioses / Luiza Galina . – 2017.

73 f.

Dissertação (Mestrado) – Programa de Pós-Graduação em Biologia Celular e Molecular, PUCRS.

Orientador: Prof. Dr. Luiz Augusto Basso.

1. Leishmania braziliensis. 2. Purine salvage. 3. Adenilosuccinate lyase. 4. Biochemical characterization. 5. Cutaneous leishmaniasis. I. Basso, Luiz Augusto. II. Título.

Elaborada pelo Sistema de Geração Automática de Ficha Catalográfica da PUCRS com os dados fornecidos pelo(a) autor(a).

Luiza Galina

Caracterização bioquímica da enzima Adenilosuccinato liase de Leishmania (Viannia) braziliensis visando o planejamento racional de fármacos antileishmaniose

Dissertação de Mestrado apresentada ao Programa de Pós-Graduação em Biologia Celular e Molecular, da Faculdade de Biociências da Pontifícia Universidade Católica do Rio Grande do Sul.

Aprovado em 26 de outubro de 2017

BANCA EXAMINADORA

_____

Prof. Dr. André Arigony Souto - PUCRS

_____

Prof. Dr. Jarbas Rodrigues de Oliveira - PUCRS

_____

Prof. Dr. Mario Sérgio Palma - UNESP

Porto Alegre

2017

AGRADECIMENTOS

Gostaria de agradecer primeiramente a minha família, aos meus pais, ao meu irmão e ao meu namorado por todo o apoio e amor incondicional que sempre me deram.

Quero agradecer a todos os meus professores, especialmente aos meus orientadores, Professor Diógenes Santiago Santos (*in memoriam*) que sempre me incentivou e me deu a oportunidade de trabalhar nesse laboratório excelente com profissionais incríveis; e ao meu orientador "adotivo" Professor Luiz Augusto Basso, que tanto tem me ensinado neste curto espaço de tempo em que tem me orientado.

Agradeço a todos os professores, pesquisadores, amigos e colegas do Centro de Pesquisa em Biologia Molecular e Funcional (CPBMF) por todo o carinho, apoio, amizade e incentivo. Esse trabalho também é de vocês! Obrigada especialmente a Anne que sempre me ajudou em tudo, minha amiga e exemplo de vida!

Agradeço a todos os meus amigos, os melhores que alguém pode ter. Vicky, Bruna, Gui, Rafa, Duda e Ju, meus amados "xuxus", cúmplices que desde o primeiro semestre da faculdade sempre estiveram do meu lado, me aturando, me incentivando, me ajudando a ser uma pessoa melhor a cada dia. Amadas Cissa, Nathalia e Stefani por todo o amor, paciência, conselhos e por terem me ajudado a vencer mais essa etapa com sucesso! Eu não teria conseguido sem vocês!

Um mestrado, assim como qualquer outra grande conquista, não é possível de ser realizado sozinho. A todas as pessoas que direta ou indiretamente contribuíram para a conclusão desse trabalho e para o meu crescimento pessoal, do fundo do meu coração, muito obrigada!

Por fim, agradeço PUCRS e também pelo apoio financeiro obtido pela CAPES e BNDES.

RESUMO

A enzima Adenilosuccinato liase (ASL) pertence a superfamília de enzimas aspartase/fumarase, as quais compartilham o mecanismo catalítico ácido-básico com β-eliminação de fumarato como o produto comum. A ASL está envolvida tanto na biossíntese *de novo* quanto na via de salvamento de purinas. Aqui são descritos os métodos de clonagem, expressão e obtenção da proteína recombinante ASL de *Leishmania* braziliensis (*Lb*ASL) na sua forma homogênea. Análises da proteína recombinante por espectrometria de massa, determinação do estado oligomérico e alinhamento múltiplo de sequências também são apresentados. Ensaios de cinética em estado estacionário mostraram que a *Lb*ASL segue o perfil de Michaelis-Menten. Experimentos de titulação isotérmica por calorimetria sugerem que a *Lb*ASL segue um mecanismo cinético Uni-Bi ordenado, no qual o fumarato é liberado primeiro do sítio ativo seguido pelo AMP. Dados de velocidade iniciais para a reação reversa e a relação de Haldane permitiram calcular uma constante de equilíbrio desfavorável para a reação química catalisada pela enzima. Os parâmetros de energia de ativação e termodinâmica também foram estimados. Os efeitos isotópicos do solvente *V/K* e *V* sugerem uma modesta contribuição da transferência de prótons do solvente durante o passo limitante da reação. Os dados obtidos no inventário de prótons mostram um modesto efeito em *V* resultante de um único sítio protônico, e o valor de transição do fator de estado de fracionamento de 0,74 sugere a participação da transferência de prótons do solvente em vibrações de estado de transição perpendiculares à coordenada da reação. Experimentos de perfil de pH para k_{cat} e k_{cat}/K_M sugerem os resíduos de aminoácidos envolvidos, respectivamente, na catálise e ligação do substrato. A modelagem molecular para *Lb*ASL foi realizada visando prover uma base estrutural para interpretação dos dados experimentais. Um melhor entendimento do modo de ação da *Lb*ASL será útil para o desenho racional de agentes antileishmanioses.

Palavras chave: *Leishmania braziliensis*, salvamento de purinas, adenilossucinato liase, caracterização bioquímica, leishmaniose cutânea.

ABSTRACT

Adenylosuccinate lyase (ASL) belongs to aspartase/fumarase superfamily of enzymes which share a general acid-base catalytic mechanism with β-elimination of fumarate as common product. ASL is involved in both de novo and salvage pathways of purine biosynthesis. Cloning, expression, and a method to obtain homogeneous recombinant ASL from Leishmania braziliensis (*Lb*ASL) are described. Mass spectrometry analysis of recombinant *Lb*ASL, oligomeric state determination and multiple sequence alignment are presented. Steady-state kinetics of *Lb*ASL showed a Michaelis-Menten pattern. Isothermal titration calorimetry binding assays suggested that *Lb*ASL follows a Uni-Bi ordered kinetic mechanism, in which release of fumarate is followed by AMP to yield free enzyme. Initial velocity data for the reverse reaction and the Haldane relationship allowed calculation of an unfavorable equilibrium constant for *Lb*ASL-catalyzed chemical reaction. The activation energy and thermodynamic activation parameters were estimated. Solvent kinetic isotope effects *V/K* and *V* suggest a modest contribution of solvent proton transference during the rate-limiting step of the reaction. Proton inventory data show that the modest normal effect on *V* arises from a single protonic site, and the transition state fractionation factor value of 0.74 suggests participation of solvent proton transfer in transition-state vibrations perpendicular to the reaction coordinate. pH-rate profiles for k_{cat} and k_{cat}/K_M suggested amino acid residues involved in, respectively, catalysis and substrate binding. A model of *Lb*ASL was built to provide a structural basis for the experimental data. A better understanding of the mode of action of *Lb*ASL is useful for the rational design of antileishmaniasis agents.

Keywords: *Leishmania braziliensis*, purine salvage, adenylossucinate lyase, biochemical characterization, cutaneous leishmaniasis.

LISTA DE ABREVIATURAS E SIGLAS

LC – Leishmaniose cutênea

LV – Leishmaniose visceral

LCL – Leishmaniose cutânea localizada

LCD – Leishmaniose cutânea difusa

LM – Leishmaniose mucocutânea

OMS – Organização Mundial da Saúde

ATP – Adenosina trifosfato

GTP – Guanosina trifosfato

Sb^{+} - Antimonial pentavalente

AmB – Amfotericina B

GM-CSF – Fator estimulante de colônias de granulócitos e macrófagos

DNA – Ácido desoxirribonucleico

RNA – Ácido ribonucleico

PRPP – 5-fosforibosil-1-pirofosfato

IMP – Inosina monofosfato

AMP – Adenosina monofosfato

GMP – Guanosina monofosfato

XMP – Xantosina monofosfato

PRTases – Enzimas fosforibosiltransferases

APRTase – Adenina fosforibosiltransferase

HGPRTase – Hipoxantina-guanina fosforibosiltransferase

XPRTase – Xantina fosforibosiltransferase

IMPDH – inosine monofosfato desidrogenase

ADSS – Adenilosuccinato sintetase

ASL – Adenilosuccinato liase

GMPS – Guanosina monofosfato sintetase

GMPR – Guanosina monofosfato redutase

SAICAR – 5-aminoimidazol-(N-succinilocarboxamida) ribonucleotideo

AICAR – 5-aminoimidazol-4-carboxamida ribonucleotideo

S-AMP – Adenilosuccinato

*Lb*ASL – Adenilosuccinato liase de *Leishmania braziliensis*

ITC – Calorimetria de titulação isotérmica

LISTA DE ILUSTRAÇÕES

SUMÁRIO

Capítulo 1

Capítulo 2

Capítulo 3

Capítulo 1

Introdução

Justificativa

Objetivos

1. INTRODUÇÃO

1.1. Leishmaniose - Aspectos gerais

A leishmaniose é uma doença infecciosa, não contagiosa, causada por protozoários da família Trypanosomatidae, do gênero *Leishmania*. A doença é considerada um importante problema de saúde pública, sendo umas das principais doenças negligenciadas [1,2]. Em humanos, a infecção por *Leishmania* pode causar várias síndromes clínicas com comprometimento da pele, mucosas das vias respiratórias superiores e vísceras [3]. As leishmanioses são classificadas como Leishmaniose cutânea (LC), que engloba as formas cutâneas e mucocutânea da doença, e a Leishmaniose Visceral (LV), também chamada de Kala-azar [4,5].

A LC possui três manifestações clínicas distintas: Leishmaniose Cutânea Localizada (LCL) – caracterizada por lesões cutâneas, geralmente indolores, ulceradas ou não, com bordas elevadas, de fundo granuloso e avermelhado; Leishmaniose Cutânea Difusa (LCD) - assemelha-se a LCL, porém apresenta lesões infiltradas e disseminadas por todo o corpo; e Leishmaniose Mucocutânea (LM) – na maioria dos casos, uma evolução secundária da forma cutânea, caracterizada pela formação de lesões desfigurantes e destrutivas na boca, nariz, palato, faringe e laringe, podendo causar mutilações na face [1,4,6,7,8,9]. Por fim, a Leishmaniose Visceral (LV), é a forma mais severa da doença, acometendo as vísceras como fígado, baço, medula óssea e linfonodos, podendo levar a morte do paciente [4,8,9,10].

Dentre os fatores de risco que facilitam a transmissão da doença, destacam-se a condição socioeconômica da população, a mobilidade e as mudanças ambientais e climáticas. Os diferentes padrões de transmissão e o conhecimento ainda limitado sobre alguns aspectos, como a mobilidade da população e dos reservatórios naturais do parasito, torna difícil o controle da doença [1,3,6].

Todas as espécies de *Leishmania* são transmitidas pelas fêmeas de dípteros da subfamília Phlebotominae, pertencentes aos gêneros *Lutzomyia* e *Psychodopigus* no continente americano, e *Phlebotomus* no continente europeu. No Brasil, mosquitos do gênero *Lutzomyia,* conhecidos popularmente como

mosquito palha, tatuquira, birigui, entre outros, são de fácil identificação devido a sua coloração castanho-claro e por manter as asas eretas quando pousa [6,13]. O papel vetorial de cada espécie do mosquito dependerá da espécie de *Leishmania* presente no intestino do vetor [6].

No Brasil, foram identificadas sete espécies de *Leishmania*, sendo seis do subgênero *Viannia* e uma do subgênero *Leishmania*. As três principais espécies são: *Leishmania* (*Vianna*) *braziliensis*, *L*. (*V*.) *guyanensis* e *Leishmania* (*Leishmania*) *amazonensis* e, mais recentemente, as espécies *L*. (*V*.) *lainsoni*, *L*. (*V*.) *naiffi*, *L*. (*V*.) *lindenberg* e *L*. (*V*.) *shawi* foram identificadas em estados das regiões norte e nordeste [6,13].

Segundo a Organização Mundial da Saúde (OMS) a leishmaniose é endêmica em 98 países, sendo que aproximadamente 0,2 a 0,4 milhões de novos casos de leishmaniose visceral (LV) e 0,7 a 1,2 milhões de novos casos de leishmaniose cutânea (LC) ocorram anualmente. No Brasil, predominam as formas de LC e mucocutânea; porém, a LV apresenta alta taxa de mortalidade [4,11]. Segundo o Ministério da Saúde no ano de 2016 ocorreram mais de 12 mil casos de LC e cerca de 3 mil casos de LV, sendo as regiões norte mais afetada pela LC e nordeste mais afetada pela LV [12].

1.2. *Leishmania (Viannia) braziliensis*

A *Leishmania* (*Viannia*) *braziliensis* foi a primeira espécie de *Leishmania* descrita como agente etiológico da LT nas Américas e é encontrada em todas as regiões do país. Geralmente, está associada com a presença de animais domésticos e a transmissão frequentemente ocorre dentro das habitações. No homem, é a espécie mais prevalente e pode causar lesões cutâneas e mucocutâneas. A transmissão é associada aos vetores *Lutzomyia whitmani*, *L*. *migonei*, *L*. *intermedia* e *Psychodopigus wellcomei*, dependendo da região [1,6,13].

1.3. Ciclo de vida da *Leishmania*

As *Leishmania* spp. são organismos digenéticos (completam seu ciclo de vida passando por pelo menos dois hospedeiros), alternando entre as formas flageladas promastigotas no intestino de flebotomíneos e amastigota intracelular no hospedeiro mamífero [14].

A infecção das fêmeas do flebotomíneo ocorre quando estas se alimentam de sangue infectado de um hospedeiro mamífero e ingerem macrófagos contendo leishmanias na forma amastigota [4]. No trato digestório do vetor ocorre o rompimento da membrana dos macrófagos e os parasitos são liberados. Na região do intestino médio abdominal, ocorre a transformação dos amastigotas em promastigotas procíclicos, que se multiplicam através de divisão binária. Após a divisão, migram para a região anterior do intestino onde se concentram e sofrem um processo de diferenciação, denominado metaciclogênese. Nesse processo, os promastigotas apresentam redução no tamanho do corpo celular, tornam-se extremamente móveis e altamente infectivos e passam a ser denominados promastigotas metacíclicos. As formas metacíclicas migram para a probóscide e são regurgitados e transmitidos ao hospedeiro vertebrado através da picada durante o repasto sanguíneo [4, 15, 16].
Após a inoculação pela picada do inseto, as promastigotas interagem com neutrófilos, células dendríticas e, principalmente, macrófagos no local da picada. Estas células aderem as promastigotas e as fagocitam por meio de um mecanismo mediado por receptores e ligantes. Embora a fagocitose seja um mecanismo de defesa do hospedeiro, as leishmanias desenvolveram sistemas capazes de subverter a capacidade microbicida dos fagócitos. Uma vez fagocitadas, as promastigotas ficam alojadas em fagossomos. Nos macrófagos, os fagossomos se fusionam a lisossomos, formando um fagolisossomo chamado vacúolo parasitóforo [14-19].

Dentro do vacúolo parasitóforo, as promastigotas se diferenciam em amastigotas que começam a se multiplicar intensamente até romperem a célula hospedeira devido ao excesso de amastigotas [5,17,19]. Uma vez liberadas na corrente sanguínea, as amastigotas podem infectar novas células dendríticas, fibroblastos, bem como outros macrófagos [17]. O ciclo de transmissão se completa quando mosquitos não infectados ingerem sangue contendo fagócitos infectados [5]. O ciclo de vida do protozoário está ilustrado na Figura 1.

Figura 1: Ciclo de transmissão da leishmaniose em humanos.

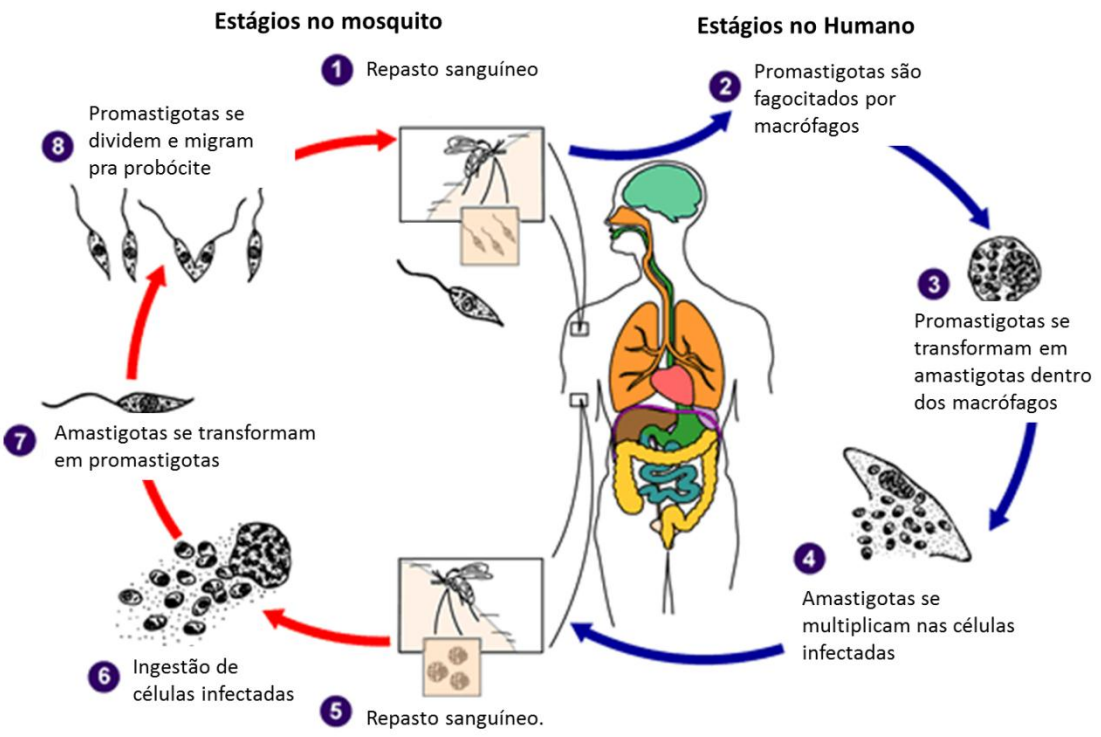

Fonte: adaptado de CDC http://www.cdc.gov/parasites/leishmaniasis/biology.html. Acesso em 17/03/2016.

1.4. Tratamento

Existem muitos tratamentos para as diversas manifestações da leishmaniose, variando de tratamentos locais nas lesões cutâneas a tratamentos sistêmicos. Desta forma, a escolha dos medicamentos de primeira e segunda linha irá depender do tipo da doença e da prática regional [20].

Os antimoniais pentavalentes (Sb^{+5}) são considerados os medicamentos de primeira linha para o tratamento das leishmanioses. A OMS recomenda a dosagem de 20 mg de Sb^{+5}/kg/dia, durante 20 dias seguidos, podendo ser utilizado o antimoniato de N-metilglucamina ou estibogluconato de sódio, sendo que apenas o primeiro é disponibilizado no Brasil pelo Ministério da Saúde[6]. Estes medicamentos interferem nas vias bioenergéticas de *Leishmania* na forma amastigota, inibindo a glicólise e oxidação de ácidos graxos, reduzindo a produção de ATP e GTP. No entanto, o mecanismo de ação preciso ainda está

sendo investigado [20,21]. As grandes desvantagens destes medicamentos são o custo elevado e a alta toxicidade, que pode provocar deficiência ou falência renal, alterações hepáticas e cardiológicas, além de febre, enjoos e náuseas. Devido ao seu potencial teratogênico, não há possibilidade de administração em gestantes. Os Sb^{+5} são administrados via parenteral, sendo necessária a administração em âmbito hospitalar e um cuidadoso monitoramento dos pacientes durante o tratamento. Estes fatores contribuem para a baixa aderência ao tratamento ou interrupção do mesmo, o que favorece a seleção de parasitas com resistência ao medicamento [20-22].

A anfotericina B (AmB) é o medicamento de primeira linha para gestantes e o de segunda linha mais utilizado quando o tratamento com os Sb^{+5} não apresentam resultados. O mecanismo de ação da AmB causa a instabilidade e ruptura da membrana citoplasmática do protozoário. Recomenda-se a dosagem de 0,5 mg/Kg/dia, aumentando gradualmente até 1 mg/Kg/dia por no mínimo 20 dias, em dias alternados. Os efeitos adversos mais frequentes são febre, náuseas, vômitos, hipopotassemia, flebite no local da infusão e deficiência renal. Embora seus efeitos colaterais sejam menos agressivos do que os Sb^{+5}, o tratamento é mais longo e também requer administração e acompanhamento em âmbito hospitalar. A anfotericina na forma lipossomal é menos tóxica, porém o custo elevado restringe seu uso em regiões onde a doença é endêmica [6,20-24].

Miltefosina é o medicamento mais recente lançado no mercado e o único para tratamento oral de leishamaniose visceral. Também mostrou resultados positivos para LC causada por *L*. *mexicana*, *L*. *guyanensis* e *L*. *panamensis*, porém é ineficaz contra lesões causadas por *L*. *braziliensis*. Embora este medicamento não apresente muitos efeitos colaterais, possui efeitos teratogênicos [20].

Tratamentos tópicos realizados com imiquimoda e paromomicina aplicadas nas lesões, têm mostrado resultados positivos para tratar LC em conjunto com outros medicamentos sistêmicos [20-22]. Outros estudos demonstram que o uso tópico de fator estimulante de colônias de granulócitos e macrófagos (GM-CSF), adicionado ao tratamento padrão com antimoniais, acelera a cicatrização das lesões [25,26]. Terapias utilizando calor a 50°C aplicado diretamente nas lesões de LC são uma opção para pacientes HIV-positivos, nos quais os tratamentos de primeira e segunda linha não apresentam resultados

[20,27]. Recentemente, um candidato a vacina utilizando nanopartículas contendo um conjugado polivalente do trissacarídeo α-Gal em partícula viral Qβ (Qβ−α-Gal nanopartículas) foi testado em modelos de camundongos *knockout* para o gene C57BL/6 α-galactosiltransferase, apresentando resultados promissores na eliminação da infecção e proliferação de *L. amazonensis* e *L. infantum*, espécies causadoras de LC e LV, respectivamente [28].

Diante deste panorama, é de suma importância continuar os esforços para planejamento e desenvolvimento de novos medicamentos eficientes contra a leishmaniose, que sejam menos tóxicos, de fácil administração e de custo reduzido [5, 20,23].

1.5. Planejamento racional de novos fármacos contra *Leishmania* – Metabolismo de Purinas

O planejamento racional de fármacos, usualmente, baseia-se em explorar as diferenças bioquímicas e fisiológicas entre o patógeno e seus hospedeiros. A identificação dessas diferenças metabólicas possibilita a seleção de potenciais alvos moleculares para ação de novos inibidores [29,30,31]. Algumas diferenças metabólicas interessantes entre a *Leishmania* e seus hospedeiros mamíferos são encontradas no metabolismo de nucleotídeos de purinas [30]. Esses nucleotídeos, além de serem as unidades monoméricas precursoras de DNA e RNA, também exercem importantes funções como moduladores de atividades enzimáticas e como constituintes de algumas coenzimas, onde estão envolvidas em reações de liberação de açúcares e transferência de energia [32,33]. Em mamíferos, os nucleotídeos de purina são obtidos através de duas rotas distintas: a via de biossíntese *de novo* e a via de salvamento [33]. Entretanto, os protozoários da família Trypanosomatidae, na qual *Leishmania* está inserida, não possuem a via de biossíntese *de novo*, sendo totalmente dependentes da via de salvamento de purinas para a obtenção destes nucleotídeos [34].

Na via de biossíntese *de novo*, o anel purínico é montado a partir de vários precursores simples como a glicina, o aspartato e a glutamina. A porção ribose fosfato dos nucleotídeos purínicos é obtida a partir do 5-fosforribosil-1-pirofosfato (PRPP) sintetizado a partir de adenosina trifosfato (ATP) e 5-fosforribose. De modo geral, a via consiste na adição progressiva de átomos formadores do anel

purínico ao carbono 1 da 5-fosforribose em onze etapas dependentes de ATP, cujo primeiro produto formado é o ribonucleotídeo de hipoxantina ou inosina monofosfato (IMP). O IMP constitui um composto-chave na sequência metabólica dos ribonucleotídeos de purinas, podendo ser convertido em adenosina monofosfato (AMP) ou guanosina monofosfato (GMP) através de duas vias distintas. O AMP é sintetizado a partir do IMP por uma via de duas reações. Na primeira reação, o grupo amino do aspartato é ligado ao IMP que produz adenilosuccinato. Na segunda reação, a enzima adenilosuccinato liase catalisa a eliminação do fumarato do adenilosucinato para formar o AMP. A mesma enzima catalisa a nona etapa da síntese de IMP. O GMP também é formado a partir de uma rota com duas reações. Primeiramente, o IMP é desidrogenado formando xantosina-monofosfato (XMP), após o XMP é convertido em GMP pela transferência do nitrogênio amídico da glutamina em uma reação promovida pela hidrólise de ATP a AMP+PP_i (Figura 2 e 3) [35-38].

Figura 2: Esquema representativo da síntese de inosina monofosfato pela biossíntese *de novo* de purinas.

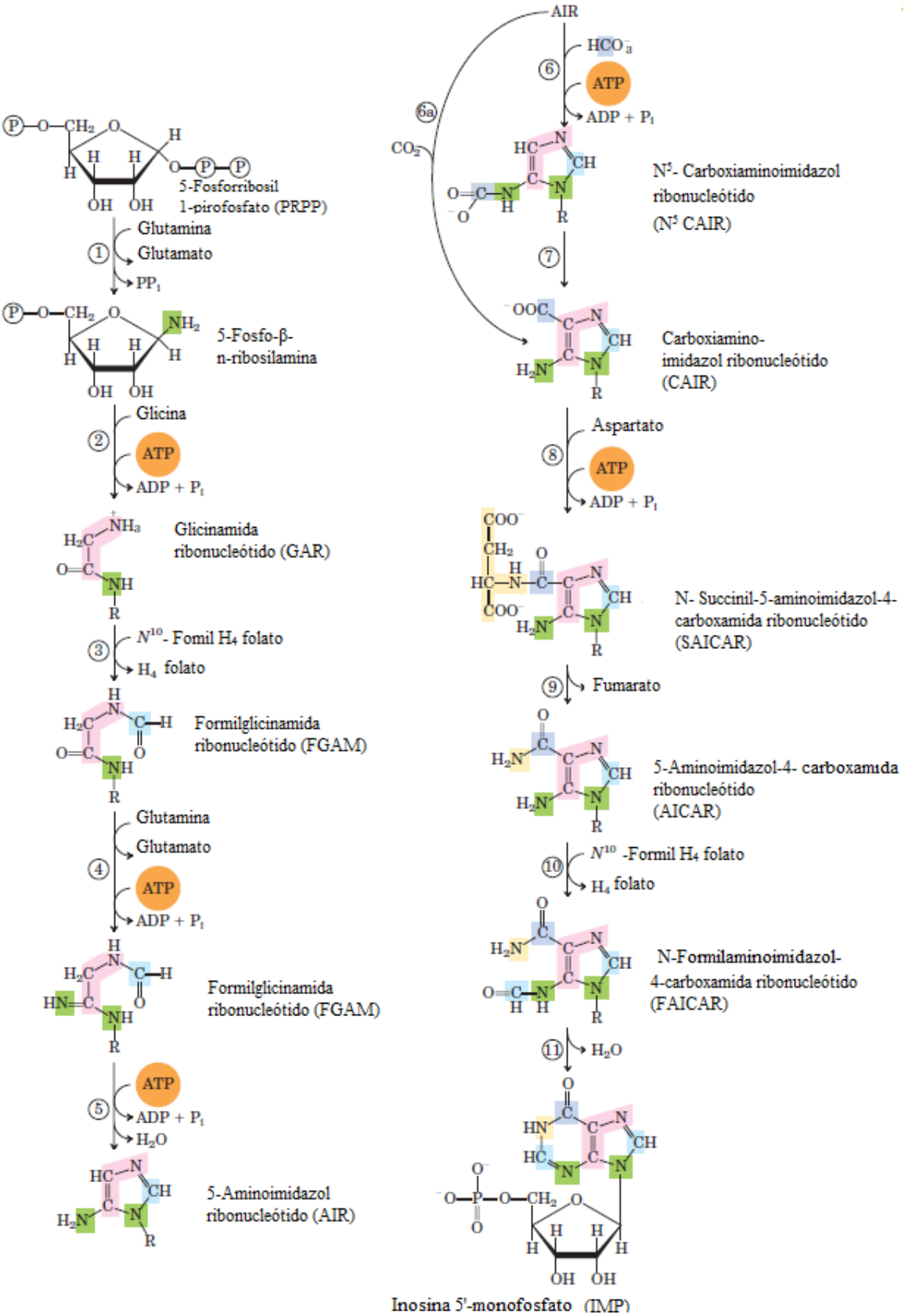

Fonte: Adaptado de Voet *et al*. 2006

Figura 3: IMP é convertido em AMP e GMP em duas reações separadas na mesma rota.

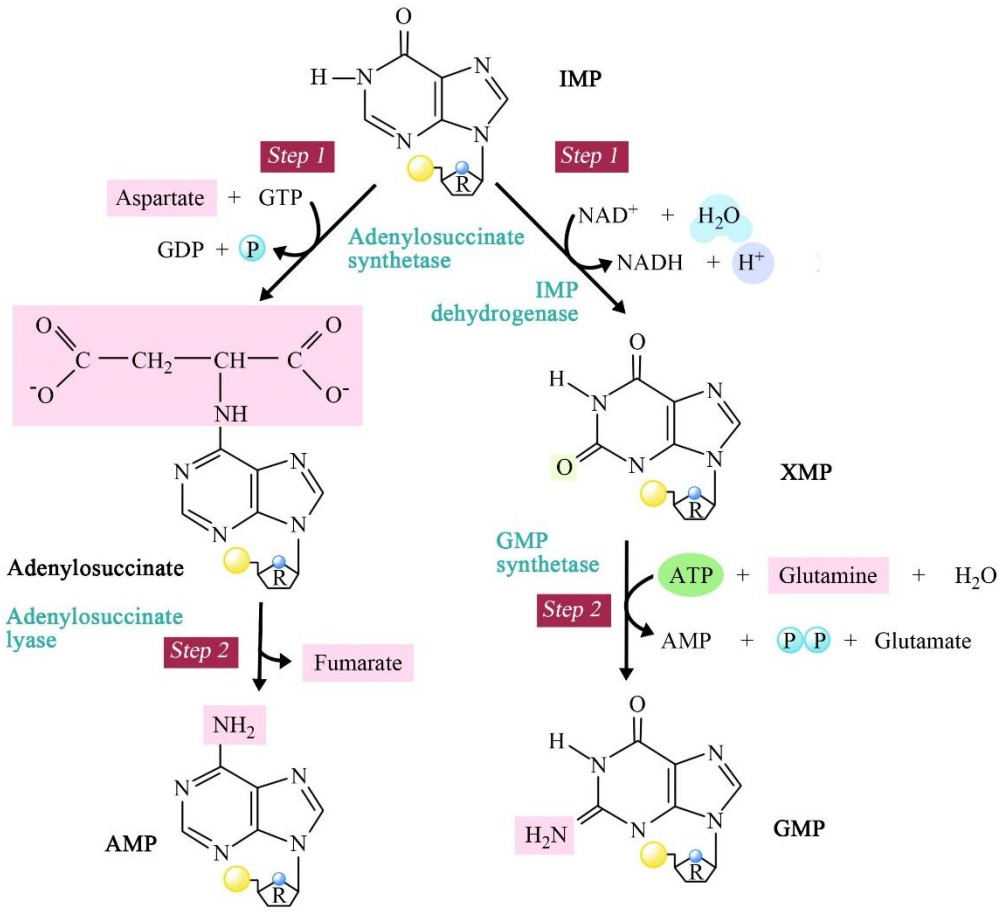

Fonte: Adaptado de Voet *et al*. 2006.

A via de salvamento de purinas é mais simples e menos dispendiosa comparada a biossíntese *de novo*. Nesta via, ocorre a recuperação de purino-nucleotídeos pré-formados como adenina, guanina e hipoxantina livres resultantes da degradação de ácidos nucleicos ou de nucleotídeos livres, através da reação direta do PRPP com as purinas livres, que são convertidas em IMP, AMP e GMP pela ação de enzimas fosforibosiltransferases (PRTases) correspondentes [37,38].

Uma vez que *Leishmania* não é capaz de realizar a biossíntese *de novo* de purinas, estes organismos possuem uma extensa via de salvamento de purinas que lhes permite reutilizar purinas de seu meio de cultura ou do hospedeiro, sendo capazes de incorporar nucleosídeos ou nucleobases purínicas [33,36,39,40]. Enquanto mamíferos possuem duas enzimas PRTases específicas, a adenina fosforribosiltransferase (APRTase) e a hipoxantina-

guanina fosforribosiltransferase (HGPRTase), protozoários do gênero *Leishmania* possuem além destas duas enzimas, uma terceira PRTase exclusiva para xantina (XPRTase) [32,35,36]. O salvamento de purinas é similar nas formas amastigotas e promastigotas, diferindo apenas no metabolismo de adenina e adenosina. Em promastigotas, praticamente toda a adenina é convertida em hipoxantina pela catálise de uma adenina deaminase. Em amastigotas não há adenina deaminase, sendo que a adenina é convertida em AMP pela ação direta da APRTase [32].

Estudos realizados em *L. donovani* mostraram que o fluxo majoritário na via de salvamento está na conversão de IMP em AMP e XMP em GMP, sugerindo que as enzimas de interconversão de nucleotídeos como a inosina monofosfato desidrogenase (IMPDH), adenilosuccinato sintetase (ADSS), adenilosuccinato liase (ASL), GMP sintetase (GMPS), GMP redutase (GMPR) e AMP deaminase são essenciais para o parasito [39] (Figura 4).

Figura 4: Esquema representativo da rota de salvamento de purinas em *Leishmania*.

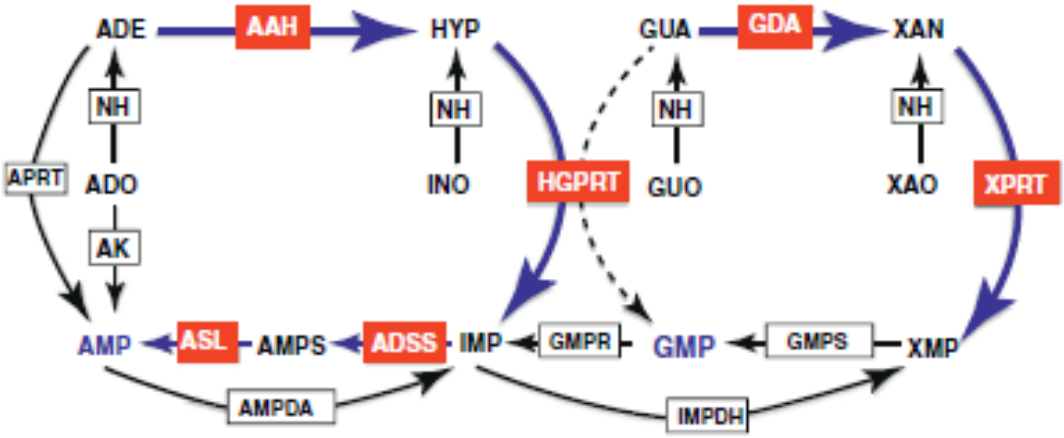

Figura 4: Flechas azuis representam o fluxo majoritário de substratos na via de salvamento de purinas. As menores atividades estão representadas pelas flechas pretas, e a linha tracejada representa a fosforibosilação de guanina que raramente ocorre em *Leishmania*. Abreviações: APRT, adenina fosforribosiltransferase, HGPRT, hipoxantina-guanina fosforribosiltransferase, XPRT, xantina fosforribosiltransferase, AK, adenosina quinase, AAH, adenina aminohidrolase, GDA, guanina deaminase, ADSS, adenilosuccinato sintetase, ASL, adenilosuccinato liase, AMPDA, adenosina monofosfato deaminase, IMPDH, inosina monofostafase desidrogenase, GMP, guanosina monofosfato sintetase, GMPR, guanosina monofosfato redutase, NH, nucleosídeo hidrolase, ADO, adenosina, INO, inosina, HYP, hipoxantina, GUO, guanosina, GUA, guanina, XAO, xantosina, XAN, xantina. Fonte: adaptado de Jan M. Boitz *et al*. 2012.

A importância das vias de interconversão de nucleotídeos para o crescimento e para o potencial de infecção já foi validada através de experimentos de isolamento e caracterização de cepas *L. donovani* mutantes com ausência dos genes funcionais de ADSS, ASL e IMPDH [41,42]. Os três mutantes apresentaram fenótipos de infecciosidade reduzida em macrófagos; no entanto, apenas parasitas nocautes para ASL foram severamente incapacitados na sua habilidade de estabelecer uma infecção visceral em camundongos comparado com os outros genes nocautes. Outro estudo com *L. donovani* também demonstrou a relevância da enzima GMPR para a produção de nucleotídeos [43]. Neste cenário, a via de salvamento de purinas apresenta alvos potenciais para planejamento de inibidores eficientes contra o *Leishmania* [39,44].

1.6. Enzima adenilosuccinato liase

A ASL é uma enzima *housekeeping* encontrada em muitos organismos, possui um papel importante na replicação celular, na produção de purinas e no metabolismo celular. É a única enzima que está presente em ambas as rotas do metabolismo de purinas catalisando duas reações distintas, não sequenciais e com substratos específicos [37,38].

Na biossíntese *de novo, a* ASL medeia a reação de clivagem do 5-aminoimidazol-(N-succinylocarboxamida) ribotideo (SAICAR) em 5-aminoimidazole-4-carboxamida ribotideo (AICAR) e fumarato. Na via de salvamento de purinas, a qual é funcional em *Leishmania*, a enzima catalisa a clivagem de adenilosuccinato monofosfato (S-AMP), proveniente do IMP, promovendo a formação de AMP e fumarato (Figura 5).

Figura 5: Reações catalisadas pela enzima ASL

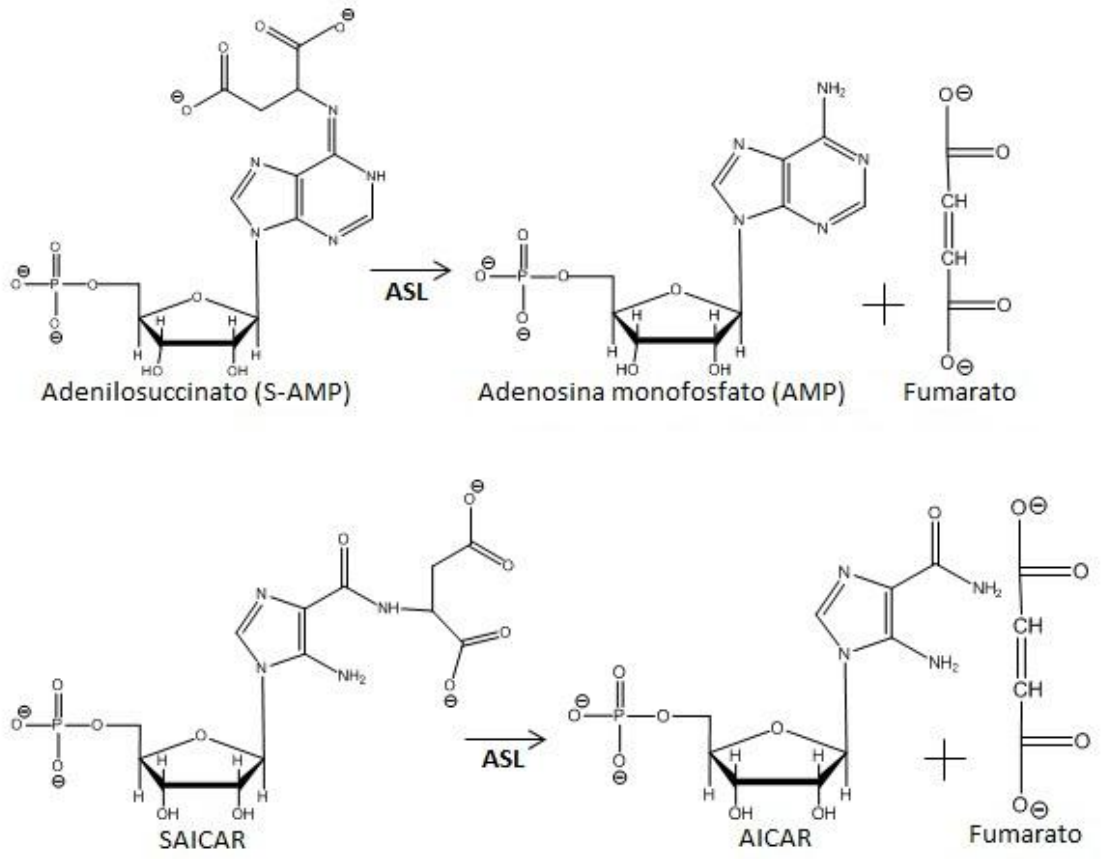

Fonte: Adaptado de Berens *et al* 1995.

O sítio ativo da enzima é o mesmo em ambas as reações [37,38,39,40,42,44,45]. Foi demonstrado que as reações envolvem uma catálise ácido-base com a β-eliminação de um grupo succinil do substrato levando a liberação do fumarato, o qual deixa o sítio ativo da enzima antes da liberação do AICAR ou AMP [45].

A sequência de aminoácidos da enzima ASL, bem como sua estrutura tridimensional e a determinação de parâmetros cinéticos já foram elucidados para uma variedade de organismos incluindo *Escherichia coli* (PDB ID: 2PTR), *Leishmania donovani* (PDB ID: 4MX2) e *Homo sapiens* (PDB ID: 2CV6), demonstrando que o sítio catalítico da enzima é conservado para todas as espécies [42-51]. A estrutura tridimensional da enzima ASL de *L. braziliensis* ainda não foi elucidada até o presente momento, no entanto, através do alinhamento das sequências de aminoácidos da enzima ASL de *L.braziliensis* e de *L. donovani*, observou-se que a ASL de *L. braziliensis* possui 88% de identidade

com *L. donovani*, cuja estrutura tridimensional já foi determinada, bem como a conservação dos resíduos de aminoácidos presentes no sítio ativo [44,48].

Estudos realizados com a ASL de *Plasmodium falciparum* demostraram tanto a capacidade de a enzima catalisar a clivagem do substrato da via *de novo* SAICAR quanto os parâmetros cinéticos e termodinâmicos semelhantes aos de S-AMP, assim como demostraram que a interação com o produto AICAR apresenta afinidade similar ao AMP. Neste estudo, o uso de AICAR apresentou atividade inibitória sobre a ASL causando redução no crescimento do parasita em cultura [52,53]. Estudos adicionais em busca de compostos que apresentem uma atividade inibitória sobre a ASL são necessários, tendo em vista que diversos trabalhos sustentam o potencial desta enzima como um alvo para desenvolvimento de fármacos anticâncer e bactericidas [30,42,45,52,54]. Portanto, a caracterização bioquímica e funcional da enzima ASL de *Leishmania braziliensis* nos trará informações adicionais que possam auxiliar no planejamento de agentes terapêuticos contra leishmaniose.

2. JUSTIFICATIVA

As leishmanioses constituem um problema mundial de saúde pública. A cada ano, cerca de 2 milhões de novos casos são registrados no mundo. No Brasil, as leishmanioses atingem grande parte da população, sendo as regiões norte e nordeste as mais afetadas.

Atualmente os medicamentos utilizados para o tratamento das leishmanioses são caros, necessitam de assistência médica para sua aplicação, apresentam alta toxicidade e efeitos colaterais severos. Tais fatores levam à baixa adesão ao tratamento, à reincidência da doença e à seleção de parasitas resistentes aos medicamentos. Diante desse panorama, o desenvolvimento de fármacos mais eficazes e menos tóxicos se faz necessário. A identificação e o entendimento das rotas metabólicas e das enzimas que são essenciais para a sobrevivência e/ou infecção do parasita representam um ponto de partida para o planejamento racional de novas classes de compostos inibidores. A via de salvamento de purinas é a única forma das leishmanias adquirirem os nucleotídeos purínicos exigidos em vários processos bioquímicos essenciais à sobrevivência e ao desenvolvimento do patógeno. A enzima adenilosuccinato liase desempenha uma função importante na rota de salvamento de purinas, o que a sugere como um alvo molecular para o desenvolvimento de fármacos antileishmaniais. Neste contexto, o estudo aprofundado de suas funções através da caracterização bioquímica e estrutural poderá auxiliar na busca por inibidores específicos.

3. OBJETIVOS

3.1. GERAL

Obtenção e caracterização enzimática da adenilosuccinato liase de *Leishmainia braziliensis* visando o planejamento racional de novos compostos candidatos a fármacos.

3.2. OBJETIVOS ESPECÍFICOS

3.2.1 Clonar o gene ASL_LbrM.04.0500, que codifica para a enzima adenilosuccinato liase de *Leishmainia braziliensis,* no vetor pET23a(+);

3.2.2 Expressar a proteína recombinante em cepas de *Escherichia coli*;

3.2.3 Estabelecer um protocolo de purificação da enzima;

3.2.4 Confirmar a identidade da ASL por espectrometria de massa;

3.2.5 Determinar os parâmetros cinéticos e termodinâmicos da enzima;

3.2.6 Determinar a estrutura tridimensional da proteína.

Capítulo 2

Artigo Científico

Artigo científico submetido ao periódico científico *RSC Advances* publicado pela *Royal Society of Chemistry* intitulado "Biochemical, thermodynamics and structural studies of recombinant homotetrameric adenylosuccinate lyase from *Leishmania braziliensis*"

22-Sep-2017

Dear Dr Basso:

TITLE: Biochemical, thermodynamics and structural studies of recombinant homotetrameric adenylosuccinate lyase from Leishmania braziliensis

Thank you for your submission to RSC Advances, published by the Royal Society of Chemistry. This is an automatic acknowledgement that you have uploaded your files to our online submission system. Your manuscript ID is: RA-ART-09-2017-010526

Your manuscript will be passed to an editor for initial assessment as soon as possible. If there are any problems with your submission we will contact you.

RSC Advances became a gold open access journal from Issue 1, 2017. If accepted, your manuscript will be published open access and the appropriate article processing charge (APC) will apply. Discounts on APC waivers are available to some authors - for more details please see: http://www.rsc.org/journals-books-databases/about-journals/rsc-advances

Please note that RSC Advances no longer publishes 'Just Accepted' manuscripts; the time between acceptance and final publication is typically less than 10 days and therefore we no longer feel this provides a significant benefit to our authors. Instead, articles are published following editing and proofing and once the final, paginated PDF is ready for publication.

Please indicate the above manuscript ID when you contact us about this submission. You can check the status of your manuscript by logging into your Author Centre (https://mc.manuscriptcentral.com/rscadv).

Do you have an ORCID iD? ORCID (Open Researcher and Contributor iD) is a unique researcher identifier that allows you to link your research output and other professional activities in a single record. We therefore encourage each researcher to sign up for their own ORCID account. Please edit your user account to link your ORCID iD or create a new one, ensuring that you have not linked your account to another researcher's ORCID iD. If your article is accepted, you may choose to have your ORCID record updated automatically with details of the publication.

We already have the following information for authors of this manuscript: Galina, Luiza - No ORCID iD Available, Dalberto, Pedro - No ORCID iD Available, Martinelli, Leonardo - No ORCID iD Available, Roth, Candida - No ORCID iD Available, Pinto, Antônio - No ORCID iD Available, Villela, Anne - No ORCID iD Available, Bizarro, Cristiano - No ORCID iD Available, Machado, Pablo - No ORCID iD Available, Timmers, Luis - No ORCID iD Available, de Souza, Osmar - No ORCID iD Available, de Carvalho Filho, Edgar - No ORCID iD Available, Basso, Luiz - http://orcid.org/0000-0003-0903-2407, Santos, Diogenes - No ORCID iD Available
If this is not how you want your name to appear on an Accepted Manuscript, please amend your ScholarOne account.

The Royal Society of Chemistry is a member of CrossCheck. Your submission may be compared against the CrossCheck database using the iThenticate plagiarism detection software. For further information, please see here: http://www.rsc.org/Publishing/Journals/guidelines/EthicalGuidelines/CrossCheck/CrossCheck.asp

Please contact us if we can be of any assistance.

Yours sincerely,
RSC Advances Editorial Office
advances@rsc.org
****

Biochemical, thermodynamics and structural studies of recombinant homotetrameric adenylosuccinate lyase from *Leishmania braziliensis*

Luiza Galina[a,b], Pedro Ferrari Dalberto[a,b] , Leonardo Kras Borges Martinelli[a], Candida Deves Roth[a], Antonio Frederico Michel Pinto[a], Anne Drumond Villela[a], Cristiano Valim Bizarro[a,b], Pablo Machado[a,b], Luis Fernando Saraiva Macedo Timmers[b,c], Osmar Norberto de Souza[a,b,c], Edgar Marcelino de Carvalho Filho[d], Luiz Augusto Basso[a,b,*] and Diogenes Santiago Santos[a,b]

[a]Centro de Pesquisas em Biologia Molecular e Funcional (CPBMF), Instituto Nacional de Ciência e Tecnologia em Tuberculose (INCT-TB), Pontifícia Universidade Católica do Rio Grande do Sul (PUCRS), 6681/92-A, TecnoPuc, Av. Ipiranga 6681, 90619-900, Porto Alegre, RS, Brazil.

[b]Programa de Pós-Graduação em Biologia Celular e Molecular, PUCRS, Porto Alegre, RS, Brazil.

[c]Laboratório de Bioinformática, Modelagem e Simulação de Biossistemas (LABIO), Pontifícia Universidade Católica do Rio Grande do Sul (PUCRS), Av. Ipiranga 6681, 90619-900, Porto Alegre, RS, Brazil.

[d]Hospital Universitário Professor Edgard Santos, Universidade Federal da Bahia, Salvador 40110160, BA, Brazil

*To whom correspondence may be addressed. Telephone/Fax: +55-51-33203629.
E-mail address: luiz.basso@pucrs.br (Luiz Augusto Basso).

Abstract

Adenylosuccinate lyase (ASL) is involved in both *de novo* and salvage pathways of purine biosynthesis. ASL belongs to argininosuccinate lyase/fumarase C superfamily of enzymes which share a general acid-base catalytic mechanism with β-elimination of fumarate as common product. Cloning, expression, and a method to obtain homogeneous recombinant ASL from *Leishmania braziliensis* (*Lb*ASL) are described. Mass spectrometry analysis of recombinant *Lb*ASL, oligomeric state determination and multiple sequence alignment are presented. Steady-state kinetics of *Lb*ASL showed a Michaelis-Menten pattern. Isothermal titration calorimetry binding assays suggested that *Lb*ASL follows a Uni-Bi ordered kinetic mechanism, in which release of fumarate is followed by AMP to yield free enzyme. Initial velocity data for the reverse reaction and the Haldane relationship allowed calculation of an unfavorable equilibrium constant for *Lb*ASL-catalyzed chemical reaction. The activation energy and thermodynamic activation parameters were estimated. Solvent kinetic isotope effects *V/K* and *V* suggest a modest contribution of solvent proton transference during the rate-limiting step of the reaction. Proton inventory data show that the modest normal effect on *V* arises from a single protonic site, and the transition state fractionation factor value of 0.74 suggests participation of solvent proton transfer in transition-state vibrations perpendicular to the reaction coordinate. pH-Rate profiles for k_{cat} and k_{cat}/K_M suggested amino acid residues involved in, respectively, catalysis and substrate binding. A model of *Lb*ASL was built to provide a structural basis for the experimental data. A better understanding of the mode of action of *Lb*ASL is useful for the rational design of antileishmaniasis agents.

Keywords: *Leishmania braziliensis*, purine salvage, adenilossucinate lyase, biochemical characterization, cutaneous leishmaniasis.

Introduction

Leishmaniasis is regarded as one of the most burdensome of the neglected tropical diseases.[1] The disease is endemic in 98 countries and three continents, and is estimated that 350 million people are at risk.[2] Approximately 0.2 to 0.4 million cases of visceral leishmaniasis (VL) and 0.7 to 1.2 million cases of cutaneous leishmaniasis (CL) occur each year. CL is more widely distributed, with about one-third of cases occurring in the Americas, the Mediterranean basin, and Western and Central Asia.[3] In Brazil, American tegumentary leishmaniasis (ATL) is predominantly caused by *Leishmania* (Viannia) *braziliensis*,[4] which is responsible for four distinct forms of ATL: localized CL, mucosal leishmaniasis (ML), disseminated leishmaniasis (DL) and diffuse CL (DCL).[5,6] As others *Leishmania* species, *L. braziliensis* is a digenetic protozoan parasite that is flagellated, extracellular promastigote in the phlebotomine sandfly vector; while it is an immotile, intracellular amastigote within phagolysosomes of macrophages of infected mammalian host.[4] The main drug treatments of leishmaniasis include pentavalent antimonials, as sodium stibogluconate (Pentostam) and meglumine antimoniate (Glucantime) (Croft et al 2011, Croft et al 2003; McGwire 2014). However, these antimonials have multiple toxicities and are increasingly ineffective due to the development of parasite resistance.[7-9] Although second-line drugs, such as amphotericin-B either as deoxycholate or liposomal form, paromomycin and miltefosine show fewer side effects;[7,10] these therapies are very expensive and are far from ideal.[11] There is thus an urgent need for new treatments to combat this disease.

The development of new effective antiparasitic drugs can be based on exploring the biochemical and physiological differences between the pathogen and its host. One of these metabolic differences lies in the biosynthesis of purine nucleotides.[12,13] While mammal cells hold the capacity to synthetize purine nucleotides by the *de novo* and salvage pathways, *Leishmania* species are completely dependent on the salvage pathway to supply their purine requirements.[14,15] The enzyme adenylosuccinate lyase (ASL; EC 4.3.2.2) belongs to the aspartase/fumarase protein superfamily, all members of which are homotetramers with approximately 200 kDa that share a high level of structural similarity.[16-19] ASL is the only enzyme in the purine nucleotide metabolism that catalyzes two distinct reactions, both involving β-elimination of fumarate: 1) conversion of 5-aminoimidazol-4(*N*-succinylcarboxamide) ribonucleotide (SAICAR) into 5-aminoimidazole-4-carboxamide ribonucleotide (AICAR) and fumarate, and 2) conversion of succinyl-adenosine monophosphate (S-AMP) into AMP and fumarate. The

latter reaction is part of the two-reaction pathway that converts inosine monophosphate (IMP) into AMP.[16] ASL is the last enzyme in the conversion of IMP to AMP in *Leishmania*, representing therefore a critical bottleneck in purine salvage (Boitz et al 2013). Previous studies showed that an *L. donovani* parasite containing the ASL gene knocked-out exhibited a severely reduced parasite burden in both macrophages and mice, which could be explained by the toxic accumulation of adenylosuccinate.[13] These results indicate that ASL could be a promising drug target for anti-leishmaniasis drug development.

Here, we describe cloning, expression and purification to homogeneity of recombinant *L. braziliensis* ASL (*Lb*ASL). Determination of the true steady-state kinetic parameters, thermodynamic constants of substrate and products interaction, pre-steady-state kinetics, energy of activation, solvent kinetic isotope effect (SKIE) and proton inventory studies are also presented. A three-dimensional model has been built to provide a structural basis for interpretation of experimental results. These results contribute to a better understanding of the mode of action of *Lb*ASL, which should inform the rational design of chemotherapeutic agents to treat leishmaniasis.

Experimental

Cloning and recombinant protein expression

The *Lb*ASL coding gene *Lb*rM.04.0500 containing *Nde*I and *Hind*III restriction sites on, respectively, the 5' and 3' ends was synthetized with signal peptide removed by Biomatik® and ligated into the pET23a(+) expression vector (pET23a(+)::*Lb*rM.04.0500), previously digested with the same restriction enzymes. The construction of pET23a(+)::*Lb*rM.04.0500 was submitted to automatic DNA sequencing to confirm identity, integrity and absence of mutations in the cloned gene.

The recombinant plasmid pET23a(+)::*Lb*rM.04.0500 was transformed into *E. coli* BL21(DE3) cells and plated on Luria-Bertani (LB) agar containing 50 μg mL^{-1} ampicillin. A single colony was inoculated into *LB* medium (50 mL) containing 50 μg mL^{-1} ampicillin and grown at 37 °C, 180 rpm, overnight. The culture (8.5 mL) was inoculated in LB medium (500 mL) with the same antibiotic concentration and grown in a shaker-incubator at 37 °C, 180 rpm. When the optical density at 600 nm (OD_{600}) reached 0.4-0.6, the cells were induced with 1 mM of isopropyl β-D-1-thiogalactopyranoside (IPTG) and harvested at 3h, 6h, 9h, 12h and 24h after induction. Cells were harvested by centrifugation at 8,000 × *g* for 30 min at 4 °C and stored at -20 °C. Frozen cell paste was

disrupted by sonication and soluble and insoluble fractions were analyzed by 12% sodium dodecyl sulfate polyacrylamide gel electrophoresis (SDS-PAGE).

Protein purification

Protein purification was performed by HPLC using an ÄKTA System (GE Healthcare® Life Sciences, Pittsburg, USA) at 4 °C. Approximately 2.8 g of frozen cells were suspended in 14 mL of 50 mM Tris HCl pH 7.5 (Buffer A), and incubated with 0.2 mg mL^{-1} lysozyme (Sigma–Aldrich) with stirring for 30 min at 4 °C. Cells were disrupted by sonication (10 pulses of 10 s each at 60% amplitude) and centrifuged at 48,000 × *g* for 30 min at 4 °C. The supernatant was treated with 1% (v/v) streptomycin sulfate for 30 min with slow stirring to precipitate nucleic acids and centrifuged at 48,000 × *g* for 30 min at 4 °C. The resulting supernatant was treated with 1.5 mM ammonium sulfate with stirring for 30 min. The fraction containing precipitated molecules was suspended with 8 mL of buffer A and loaded on a HiLoad Superdex 200 26/60 size exclusion column (GE Healthcare® Life Sciences, Pittsburg, USA), previously equilibrated with buffer A. Proteins were isocratically eluted with 1 column volume (CV) of buffer A at flow rate of 0.5 mL min^{-1}, and fractions containing the target protein were pooled and loaded on a HiLoad Q Sepharose High Performance 16/10 anion exchange column (GE Healthcare® Life Sciences, Pittsburg, USA), pre-equilibrated with buffer A. The column was washed with 7 CVs of buffer A, and the adsorbed proteins were eluted with a linear gradient (0-60%) of 25 CV of buffer A containing 1 M NaCl (buffer B) at flow rate of 1 mL min^{-1}. The fractions containing homogeneous *Lb*ASL were pooled and dialyzed against 50 mM potassium phosphate buffer pH 7.0, containing 150 mM KCl, 1 mM EDTA, 1 mM DTT and 10% glycerol (storage buffer), and stored at -20 °C. Protein concentration was determined by the method of BCA using a bovine serum albumin as standard (BCA protein Assay Kit, Thermo Scientific Pierce).

LbASL identification by mass spectrometry

The homogeneous protein was submitted to shotgun proteomics to confirm the enzyme's identity. In-gel digestion was performed according to Shevchenko *et al.*[20] Tryptic digest of *Lb*ASL was separated on a homemade 20 cm reverse-phase column (5 µm ODSAQ C18, Yamamura Chemical Lab, Japan) using a nanoUPLC (nanoLC Ultra 1D plus, Eksigent, USA) and eluted directly to a nanospray ion source connected to a hybrid mass spectrometer (LTQ Orbitrap Discoverty, Thermo, USA). The flow rate was

set to 300 mL min^{-1} in 120 min reverse-phase gradient. The mass spectrometer was operated in a data-dependent mode, with full MS1 scan collected in the Orbitrap, with m/z range of 400-1600 at 30,000 resolution. The eight most abundant ions per scan were selected to CID MS2 in the ion trap. Mass spectra were analyzed using PatternLab platform. MS2 spectra were searched with COMET[21] using a non-redundant database containing forward and reverse *E. coli* DH10B reference proteome and the sequence of *Lb*ASL. The validity of the peptide-spectra matches (PSMs) generated by COMET was assessed using Patternlab's module SEPro[22] with a false discovery rate of 1% based on the number of decoys.

Oligomeric state determination

An estimate for the molecular mass of *Lb*ASL in solution was obtained by injecting 100 µL of protein suspension (7 µM homogeneous *Lb*ASL in 50 mM Tris HCl pH 7.5 containing 200 mM NaCl) into a HighLoad 10/30 Superdex-200 column (GE Healthcare), and isocratically eluted with 1 CV of 50 mM Tris HCl pH 7.5 containing 200 mM of NaCl at 0.4 mL min^{-1}.

Protein elution was monitored at 215, 254 and 280 nm. The low molecular weight (LMW) and high molecular weight (HMW) Gel Filtration Calibration Kits (GE Healthcare) were used to prepare a calibration curve, measuring the elution volumes (V_e) of several standards (ferritin, aldolase, ovalbumin, conalumin, ribonuclease and carbonic anhydrase A). These values were used to calculate their partition coefficient (K_{av}, Eq. 1). Blue dextran 2000 (GE Healthcare) was used to determine the void volume (V_0). V_t is the total bead volume of the column. The K_{av} value for each protein was plotted against their correspondent molecular mass to obtain an estimate for *Lb*ASL molecular mass in solution.

$$K_{AV} = \frac{V_e - V_0}{V_t - V_0} \qquad \text{Equation 1}$$

Multiple sequence alignment and homology modeling

Multiple alignment was carried out to compare amino acid sequences of homologous ASL proteins whose residues in the active site were determined by mutagenesis studies or for which three-dimensional structures were solved. The following proteins were included in the alignment: *Leishmania braziliensis* (*Lb*ASL, XP_001561734), *Leishmania donovani* (*Ld*ASL, XP_003858107), *Escherichia coli* (*Ec*ASL, WP_000423742), *Plasmodium falciparum* (*Pf*ASL, XP_001349577), *Bacillus subtilis* (*Bs*ASL, WP_003233955), *Homo sapiens* (*Hs*ASL, NP_000017), *and Mycobacterium tuberculosis* (*Mt*ASL, WP_003898583). The alignment was performed by ClustaW[23] using the Blosum62 matrix.

Homology modelling approach, implemented in the MODELLER (Sali and Blundell, 1993) 9v19 program, was used to build a model of *Lb*ASL. The structure of ASL from *E.coli* (PDB ID: 2PTQ) associated with AMP and fumarate products was used as template. The protocol used to perform the molecular modelling experiments generated 10 models. All models were submitted to the DOPE energy scoring function[24] implemented in the MODELLER 9v19 aiming to select the best structures. The MOLPROBITY webserver[25] and PROCHECK[26] were used to verify and validate the stereochemical quality of the models.

*Steady-state kinetic parameters of Lb*ASL

Recombinant *Lb*ASL enzyme activity was monitored by a continuous assay in a UV-2550 UV/Visible spectrophotometer (Shimadzu) equipped with a temperature-controlled cuvette holder, using 1.0 cm path length quartz cuvettes. The enzyme was preincubated for 30 min at 25 °C in storage buffer. All the assays were performed under initial rate conditions at 25 ºC in 50 mM Tris HCl pH 7.5 containing 200 mM NaCl and 5 mM EDTA (buffer C), in a total volume of 0.5 mL and reaction course data collected for 60 s. The kinetic data were determined using the difference in absorption between S-AMP and AMP measuring the decrease in absorbance at 282 nm using a difference extinction coefficient value of 10,000 M^{-1} cm^{-1}. One unit of enzyme activity (U) was defined as the amount of enzyme catalyzing the conversion of 1 μmol of substrate into products per second at 25 °C.

The initial velocity study was carried out to determine the steady-state kinetic parameters for S-AMP conversion into AMP and fumarate (forward reaction). The saturation curve was performed at varying concentrations of S-AMP (5 – 100 μM) and

the reaction was initiated by the addition of the recombinant *Lb*ASL (30 nM). Hyperbolic saturation curves were analyzed by non-linear regression of data fitting to the Michaelis–Menten equation (Eq. 2), in which *v* is the steady-state velocity, *V* is the maximal velocity, *A* is the substrate concentration, and K_M is the Michaelis–Menten constant.

$$v = \frac{VA}{K_M + A} \qquad \text{Equation 2}$$

The k_{cat} values were calculated from Eq. 3, in which $[E]_t$ corresponds to the total concentration of enzyme subunits.

$$k_{cat} = \frac{V}{[E]_t} \qquad \text{Equation 3}$$

The initial velocities for the reverse reaction were determined varying the concentration of AMP (10 – 800 µM) at varied-fixed fumarate concentration (100 – 900 µM). All reactions started with addition of recombinant *Lb*ASL, assayed under standards conditions, and all measurements were performed at least in duplicates. Data from initial velocity measurements showing a pattern of lines intersecting to the left of the *y*-axis in the double-reciprocal plots (or Lineweaver–Burk plots) were fitted to Eq. 4, which describes a sequential substrate binding and ternary complex formation (reverse reaction).

$$v = \frac{VAB}{K_{ia}K_b + K_aB + K_bA + AB} \qquad \text{Equation 4}$$

For Eq. 4, *v* is the initial velocity, *V* is the true maximal initial velocity, *A* and *B* are the concentrations of the substrates (AMP and fumarate) for the reverse reaction, K_a (K_q) and K_b (K_p) are their respective Michaelis-Menten constants, and K_{ia} (K_{iq}) is the dissociation constant for enzyme-substrate *A* binary complex formation (enzyme-AMP binary complex formation for the reverse reaction).

The initial velocities for the reverse reaction were employed to calculate the equilibrium constant (K_{eq}) using the Haldane equation for an ordered Uni-Bi (or Bi-Uni) mechanism (Eq. 5). V_f is the maximal initial velocity for the forward and V_r for the reverse reaction, K_p represents the Michaelis-Menten constant for the first product to be released

from the ternary complex (fumarate), K_a represents the Michaelis-Menten constant for S-AMP (K_M of Eq. 2), and K_{iq} represents the dissociation constant for enzyme-AMP binary complex formation for the reverse reaction.[27]

$$K_{eq} = \frac{V_f K_{iq} K_p}{V_r K_a} \qquad \text{Equation 5}$$

Isothermal titration calorimetry (ITC)

ITC experiments were carried out using an iTC_{200} Microcalorimeter (Microcal, Inc., Northampton, MA). The reference cell (200 µL) was loaded with water during all the experiments and the sample cell (200 µL) was filled with recombinant *Lb*ASL at a concentration of 72 µM in buffer C. The injection syringe (39.7 µL) was filled with either AMP (2 mM) or fumarate (2 mM) in the same buffer, and the ligand binding isotherms were measured by direct titration (ligand into macromolecule). The stirring speed was 500 rpm at 25 °C and constant pressure. Titration first injection (0.5 µL) was not used in data analysis and was followed by 19 injection of 2 µL each at 300 s intervals. Control titrations (ligand into buffer) were performed in order to subtract the heats of dilution prior to data analysis. The Gibbs free energy (ΔG) of binding was calculated using the relationship described in Eq. 6, in which R is the gas constant (1.987 cal K^{-1} mol^{-1}), T is the temperature in Kelvin (T = °C + 273.15), and K_a is the association constant at equilibrium. The entropy of binding (ΔS) can also be determined by this mathematical formula. ΔH represents the enthalpy of binding. The dissociation constant at equilibrium, K_d, was calculated as the inverse of K_a (Eq. 7). All data were evaluated utilizing the Origin 7 SR4 software (Microcal, Inc.)

$$\Delta G^0 = -RT \ln K_a = \Delta H^0 - T\Delta S^0 \qquad \text{Equation 6}$$

$$K_d = \frac{1}{K_a} \qquad \text{Equation 7}$$

Energy of activation

To determine the energy of activation (E_a) of *Lb*ASL for the forward reaction, the dependence of k_{cat} on temperature was measured. Initial velocities were measured in the presence of saturating concentrations of S-AMP (100 µM) at temperatures varying from 15 to 40 °C (from 288.15 to 313.15 K). Prior to data collection, *Lb*ASL was incubated for

several minutes at all tested temperatures and assayed under standards conditions to ascertain enzyme stability is maintained. All assays were performed in duplicates. E_a was calculated from the slope (E_a/R) of the Arrhenius plot fitting the data to Eq. 8, in which R is the gas constant (8.314 J mol^{-1} K^{-1}), and A is the Arrhenius constant, which represents the product of the collision frequency (Z), and a steric factor (p) based on the collision theory of enzyme kinetics.[28,29] A simplistic approach was adopted to explain a complex phenomenon and that A is independent of temperature.

$$\ln k_{cat} = \ln A - \left(\frac{E_a}{R}\right)\frac{1}{T} \qquad \text{Equation 8}$$

The E_a value allowed to obtain an estimate for the enthalpy of activation ($\Delta H^{\#}$) employing Eq. 9. The Gibbs free energy ($\Delta G^{\#}$) of activation was estimated using Eq. 10. These values allowed to obtain an estimate for the entropy of activation ($\Delta S^{\#}$) using Eq. 11. These equations were derived from the transition state theory of enzymatic reactions.[28,29] R, E_a and T are as for Eq. 8, k_b is the Boltzmann constant (1.380658 x 10^{-23} J K^{-1}), and h is the Planck's constant (6.626075 x 10^{-34} J s^{-1}). The error in $\Delta G^{\#}$ was calculated using Equation 12.

$$\Delta H^{\#} = E_a - RT \qquad \text{Equation 9}$$

$$\Delta G^{\#} = RT\left(\ln\frac{k_B}{h} - \ln T - \ln k_{cat}\right) \qquad \text{Equation 10}$$

$$\Delta S^{\#} = \frac{\Delta H^{\#} - \Delta G^{\#}}{\mathrm{T}} \qquad \text{Equation 11}$$

$$\left(\Delta G^{\#}\right)_{Err} = \frac{RT\left(k_{cat}\right)_{Err}}{k_{cat}} \qquad \text{Equation 12}$$

Solvent kinetic isotope effects (SKIE) and proton inventory

All assays were carried out under standard reaction conditions, in duplicate. The solvent kinetic isotope effects on both *V*/*K* and *V* were determined by measuring initial velocities for *Lb*ASL reaction using varied concentrations of S-AMP in either H_2O or 90 % D_2O. The SKIE data were fitted to Eq. 13,[30] in which *V* is the maximal velocity, *A* is the substrate concentration, $E_{V/K}$ and E_V are, respectively, the isotope effect minus 1 on *V/K* and *V*, and F_i is the fraction of deuterium label in the solvent.

$$v = \frac{VA}{K\left(1 + F_i E_{V/K}\right) + A\left(1 + F_i E_V\right)} \qquad \text{Equation 13}$$

To determine the number of protons contributing to the observed solvent kinetic isotope effect, the proton inventory on the catalytic rate constant (k_{cat}) was measured at saturating concentration of S-AMP at different mole fractions of D_2O (0 - 90 %). The data for the relative activity versus mole fraction of D_2O plot were fitted to the Gross-Butler equation (Eq. 14),[30] in which k_n is the rate constant measured at various mole fractions of D_2O (e.g., k_0 = k_{cat} value in H_2O, and $k_{0.9}$ = k_{cat} value in 90 % D_2O), *n* is the isotopic composition of the solvent, and ϕ^T is the deuterium fractionation factor for transition-state proton exchange relative to bulk water (i.e., exchange equilibrium constant that measures the tendency of a transition-state site to fractionally contain deuterium versus the deuterium fraction of the solvent). It should be pointed out that Eq. 14 implies that a single proton contributes to the observed solvent isotope effect and that the reactant-state fractionation factor is equal to unity.

$$\frac{k_n}{k_0} = 1 - n + n\phi^T \qquad \text{Equation 14}$$

pH-rate profiles

Prior to carrying out pH-rate studies, *Lb*ASL was incubated for 2 min at 25 °C in 100 mM 2-(*N*-morpholino)-ethanesulfonic acid (MES)/*N*-2-hydroxyethylpiperazine-*N*-2-ethanesulfonic acid (Hepes)/2-(*N*-cyclohexylamino)-ethanesulfonic acid (CHES) buffer mixture over a wide pH range (5.0 - 10.5),[31] and assayed under standard conditions to ensure enzyme stability at the experimental pH values over the course of reaction, thereby

showing that changes in enzyme activity were due to changes in proton concentration and not to protein denaturation. Initial velocities measurements were carried out at 25 °C in solutions containing increasing concentrations of S-AMP in 100 mM MES/HEPES/CHES buffer mixture over the following pH values: 6.3 (S-AMP concentration range: 40-150 µM, [*Lb*ASL] = 60 nM), 6.5 (S-AMP concentration range: 5-60 µM with 6 or 12 nM of *Lb*ASL), 6.7 (S-AMP concentration range: 1-60 µM with 6 or 12 nM of *Lb*ASL), 7.0 (S-AMP concentration range: 5-60 µM with 6 or 12 nM of *Lb*ASL), 7.5 (S-AMP concentration range: 3-60 µM with 6 or 12 nM of *Lb*ASL), 8.0 (S-AMP concentration range: 5-60 µM with 6 or 12 nM of *Lb*ASL) , 8.5 (S-AMP concentration range: 20-180 µM with 6 or 12 nM of *Lb*ASL), 9.0-9.5 (S-AMP concentration range: 20-200 µM, [*Lb*ASL] = 12 nM). The pH-rate data for k_{cat} (Fig. 10A) were plotted to Eq. 15, in which y represents k_{cat}, C is the pH-independent plateau value of y (k_{cat}), H is the hydrogen ion concentration, and K_a and K_b are, respectively, the apparent acid and base dissociation constant for the ionizing group. Eq. 15 describes a bell-shaped pH profile for a group that must be protonated for catalysis and another group that must be unprotonated for catalysis, and participation of a single ionizing group for the acidic limb (slope value of +1) and participation of a single ionizing group for the basic limb (slope value of -1).[31]

$$\log y = \log\left(\frac{C}{1+\frac{H}{K_a}+\frac{K_b}{H}}\right) \qquad \text{Equation 15}$$

The pH-rate profile for k_{cat}/K_M was more complex (Fig. 10B). The data were tentatively either fitted to Eq. 15 or Eq. 16. The latter equation describes a bell-shaped pH profile that starts with a slope of +2 in the acidic limb which goes to an eventual slope of -1 in the basic limb, suggesting participation of two ionizing groups in the acidic limb.[31] K_0 is the product of two apparent dissociation constants. Unless the p*K*s of the groups are at least 3 pH units apart, there will not be both a linear region with a slope of +1 and a flat plateau at intermediate pH values. The intersection of the linear asymptote with slope of 2 and the poorly defined plateau will give the average of the p*K* values of the two ionizing groups.[31]

$$\log y = \log\left(\frac{C}{1+\frac{H}{K_a}+\frac{H^2}{K_0}+\frac{K_b}{H}}\right)$$ Equation 16

Results and Discussion

Cloning and recombinant protein expression

The *Lb*ASL-coding DNA sequence *Lb*rM.04.0500 was purchased from Biomatik® and cloned into the pET-23a(+) expression vector. Automated DNA sequencing confirmed the identity and the absence of mutations in the cloned fragment. The best experimental condition for *Lb*ASL protein expression was observed in competent *E. coli* BL21 (DE3) cells, in *LB* medium after 12h of growth, without IPTG induction. SDS-PAGE analysis showed that the protein was expressed in the soluble fraction of cellular extracts (~51 kDa) which is in agreement with the predicted molecular mass value of 51.269 kDa for *Lb*ASL subunit. The recombinant protein purification protocol (streptomycin sulfate and ammonium sulfate precipitations, and size exclusion and anion exchange columns) yielded approximately 20 mg from 2.8 g of frozen cells (~7 mg/g). The recombinant protein was stored at -20 °C in the storage buffer (50 mM potassium phosphate buffer pH 7.0, 150 mM KCl, 1 mM EDTA, 1 mM DTT and 10% glycerol). The storage buffer was identified as the best condition to maintain enzyme stability for up to 3 months. The recombinant enzyme lost more than 50 % of initial activity after 3 months when stored at either -20°C or -80 °C.

*Lb*ASL *identification by mass spectrometry*

The gel band of approximately 51 kDa was excised from SDS-PAGE, submitted to trypsin digestion protocol, and the peptides were analyzed by LC-MS/MS in triplicate. *Lb*ASL identity was confirmed, with the identification of 189 unique peptides and sequence coverage of 100%.

Oligomeric state determination

To determine the oligomeric state of recombinant *Lb*ASL, 100 µL was loaded on a Superdex 200 HR 10/30 size exclusion column. A single peak was obtained with elution volume corresponding to approximately 223,357 kDa, according to data fitting to Eq. 1. This molecular mass value divided by the subunit molecular mass value (51.2699 kDa)

indicates that *Lb*ASL is a homotetramer in solution. This result is in agreement with the ASL characterized previously from human[32] *L. donovani*[13] and others aspartase/fumarase superfamily members.[19]

Multiple sequence alignment and homology modeling

The multiple sequence alignment for *Leishmania braziliensis* (*Lb*ASL), *Leishmania donovani* (*Ld*ASL), *Escherichia coli* (*Ec*ASL), *Plasmodium falciparum* (*Pf*ASL), *Bacillus subtilis* (*Bs*ASL),[33,34,18] *Homo sapiens* (*Hs*ASL), and *Mycobacterium tuberculosis* (*Mt*ASL),[35] allowed to propose the likely amino acid residues involved in *Lb*ASL catalysis and substrate binding (Fig. 1). Multiple sequence alignment results showed that *Lb*ASL shares 88%, 45%, 35%, 18%, 17% and 12% sequence identity with, respectively, *L. donovani*, *E. coli*, *P. falciparum*, *B. subtillis*, *H. sapiens* and *M. tuberculosis*.

The general mechanism proposed for ASL catalysis is a β-elimination (*anti* 1,2-addition-elimination reaction), in which a general base of the enzyme abstracts the *pro-R* hydrogen from the C3 atom (Cβ) of the succinyl moiety of the substrate.[36] The resulting carbanion is stabilized as the *aci*-carboxylate (or enediolate) intermediate with two negative charges on the β-carboxylate group. Cleavage of the C-N bond of the substrate is assisted by leaving group protonation by an enzyme general acid.[19] As the reaction occurs via *anti* elimination, two separate amino acid residues for proton abstraction and donation are required. Conserved His^{141} and His^{68} in *B. subtilis* have been proposed to be, respectively, the base and acid groups.[33,37] The sequence comparison showed that residues equivalent to these histidines are conserved (Fig. 1), suggesting that His^{197} and/or His^{119} may play a role in *Lb*ALS catalysis. Alternatively, the catalytic base residue may be ascribed to Ser^{322} in *Lb*ASL (Fig. 1). Proteins belonging to the aspartase/fumarase superfamily (including ASL) share a characteristic tertiary and quaternary fold as well as similar active site architecture.[19] The monomer is comprised of three mainly α-helical domains: N-terminal (D1), central helix (D2) and C-terminal (D3). Three conserved regions are found in the D2 domain: C1 located at the start of D2, and C2 and C3 that are located in the loop regions between the helices of D2. (Fig. 2). Although spatially separated in the monomeric unit, the C1-C3 domains from three different subunits form the active site of the tetrameric polymer (Fig 2). Part of the conserved C3 region is formed by the flexible SS loop, which undergoes conformational changes upon substrate binding

that is relevant to catalysis in ASL enzymes.[37,38] The signature sequence of this SS loop in *Lb*ASL is 321GSSXXPXKXN330, and is highly conserved among all aligned sequences (Fig. 1). Site-directed mutagenesis studies on *B. subtilis* indicated that Gln^{212}, Asn^{270}, and Arg^{301} residues perform critical functions in catalysis by ASL through their contributions to the binding and orientation of the succinyl carboxylate groups of its two substrates SAICAR and S-AMP.[34] The corresponding Gln^{274}, Asn^{330} and Arg^{361} residues in *Lb*ASL are also conserved in the ASLs from other organisms (Fig 1), except Arg^{361} that is replaced with a glycine in *M. tuberculosis*.[35]

The homology model of *Lb*ASL (Fig. 3) shows a His^{197} at 4.1 Å of the C-N bond of AMP, suggesting that this residue may act as the catalytic acid. The conserved Ser^{322} is in close proximity (2.9 Å) to the C(β or α)-H bond of fumarate. This serine is in the highly conserved flexible SS loop, which closes the active site upon substrate binding. Accordingly, Ser^{322} side chain may act as the catalytic base in the *Lb*ASL reaction. Although it is tempting to suggest that the corresponding residues may play a role in *Lb*ASL mode of action, site-directed mutagenesis efforts will have to be pursued to assign any role to these amino acids.

The high conservation of key amino acid residues essential for substrate binding and catalysis for both *H. sapiens* and *L. braziliensis* ASL enzymes suggest that the development of selective inhibitors for *Lb*ASL might be challenging. Notwithstanding, a better understanding of the mode of action of *Lb*ASL may unveil differences in enzyme, chemical and catalytic mechanisms that may contribute to the development of mechanism-based anti-leishmaniasis agents.

Steady-state kinetic parameters

The initial velocity experiments were measured to obtain the true steady-state kinetics parameters and to propose an enzyme mechanism. It has been shown that *B. subtilis* ASL dissociates to a mixture of monomer-dimer-trimer with decreased enzyme activity at low temperatures (4 and 8 °C), whereas the enzyme is fully active and exists as 100% tetrameric form.[18] Accordingly, recombinant *Lb*ASL protein was preincubated for 30 min at 25 °C to ascertain maintenance of fully active tetrameric *Lb*ASL enzyme. The specific activity of *Lb*ASL was obtained by varying the concentration of S-AMP (5-100 μM) and fixed concentration of enzyme (30 nM), and measuring the decrease in absorbance at 282 nm upon S-AMP conversion into products. Substrate saturation curves were hyperbolic (Fig. 4) and the data were thus fitted to the Michaelis–Menten equation

(Eq. 2), and k_{cat} value was calculated using Eq. 3. This analysis yielded the following steady-state kinetic parameters: K_M = 10.23 (± 1.40) μM, V_{max} = 6.3 (± 0.2) U mg^{-1} and k_{cat} = 5.53 (± 0.17) s^{-1}. A comparison of the specific activity of ASL from *L. donovani*,[13,39] *P. falciparum*,[40] *H. sapiens*[32] and *M. smegmatis*[35] are summarized in Table 1. *Lb*ASL displays lower k_{cat} and specificity constant (k_{cat}/K_M) values in comparison to ASL enzymes from different species of *Leishmania* (Table 1). Interestingly, the larger overall dissociation constant (K_M) for S-AMP substrate of *Lb*ASL as compared to *H. sapiens* ASL may suggest differences from substrate binding en route to product formation that may be exploited to increase inhibitor specificity.

Table 1: Steady-state kinetic parameters for S-AMP conversion into products catalyzed by ASL homologs.

Specie	K_M (μM)	V_{max} (U mg^{-1})	k_{cat} (s^{-1})	k_{cat}/K_M (M^{-1} s^{-1})	Assay conditions
L. braziliensis	10.2 ± 1.4	6.3 ± 0.2	324 ± 10	3.2 (± 0.4) x 10^7	25º C pH 7.5
L. donovani (Spector, et al 1979)	3.3 ± 0.5	100 ± 3	87.7 ± 2.6	2.7 (± 0.4) x10^7	30°C pH 7.8
L. donovani (Boitz, et al 2013)	24.0	2.1	28	0.12 x 10^7	25°C pH 7.0
P. falciparum (Bulusu et al 2009)	32.0 ± 1.6	-	7.5 ± 0.7	0.23 (± 0.02) x 10^6	25°C pH 7.4
H. sapiens (Lee and Colman, 2007)	1.78 ± 0.05	3.88 ± 0.07	3.40 ± 0.06	1.9 (± 0.1) x10^6	25°C pH 7.4
M. smegmatis (Banerjee 2014)	43.7 ± 2.6	-	0.70 ± 0.01	1.6 (± 0.1) x 10^4	37°C pH 7.6

Double-reciprocal plots showed a family of lines intersecting to the left of the *y*-axis (Fig. 5), suggesting ternary complex formation and a sequential (either random or ordered) mechanism for the reverse reaction. The pattern of straight lines intersecting to the left of the *y*-axis rules out ping-pong (parallel lines), steady-state random (that gives non-linear reciprocal plots), and rapid-equilibrium ordered (one of the family of lines should cross at a single value on the *y*-axis) mechanisms. Accordingly, the data were fitted to Eq. 4 yielding the following values: $K_{M(AMP)}$ = 13 (± 5) μM and $K_{M(fumarate)}$ = 203 (± 20) μM, $K_{i(AMP)}$ = 112 (± 20) μM, and k_{cat} = 115 (± 3) s^{-1}. The steady-state kinetic

parameters for the forward and reverse reactions and the Haldane equation for an ordered Uni-Bi mechanism (Eq. 5) were used to calculate a value of 6280 μM (*ca* 6.3 x 10^{-6} M) for the equilibrium constant (K_{eq}). This result suggests that the forward reaction is not favorable under the *in vitro* experimental conditions here employed. However, the depletion of products in the physiological context may drive the reaction forward. At any rate, the double-reciprocal plots alone cannot distinguish between rapid-equilibrium random and steady-state compulsory ordered Bi Bi mechanisms. ITC studies were thus performed to distinguish between these enzyme mechanisms.

Isothermal titration calorimetry (ITC)

As double reciprocal plots suggested a sequential kinetic mechanism for the reverse reaction, product binding to free enzyme was assessed by ITC to ascertain the order, if any, of chemical compound interaction with free *Lb*ASL. Accordingly, binary complex formation of either AMP or fumarate binding to free *Lb*ASL enzyme was studied by ITC. No heat change was detected upon addition of fumarate, suggesting that fumarate cannot bind to free *Lb*ASL enzyme. An exothermic profile (heat release) was observed for binary complex formation upon AMP binding to free *Lb*ASL protein (Fig. 6). The ITC data yielded the following values for *Lb*ASL:AMP binary complex formation: $\Delta H°$ = -5.5 (± 1.5) kcal mol^{-1} and $\Delta S°$ = 3.13 (± 0.84) cal mol^{-1} K^{-1}. The negative enthalpy value indicates a favorable, though small, redistribution of interactomic interactions network (e.g., hydrogen bonds and/or van der Waals interactions) between the reacting species, including solvent. Hydrophobic interactions are related to the relative degrees of disorder in the free and bound systems and thus these interactions are reflected in the entropy change. The release of "bound" water molecules from a surface to the bulk solvent is usually a source of favourable entropy (positive ΔS). A reduction in conformational states in either ligand or protein upon binary complex formation is entropically unfavourable (negative ΔS) because this molecular recognition process limits the external rotational and translational freedom of both partners (for instance, structuring regions of the protein adjacent to the bound ligand and loss of conformational freedom of free ligand).[41] The positive entropy value suggests either release of bound water molecules and/or an increase in conformational states in *Lb*ASL or AMP upon binary complex formation. The Gibbs free energy $\Delta G°$ value of -5.6 (± 1.5) kcal mol^{-1} ($K_d \cong 19 \pm 7$ μM) suggests a favorable process for *Lb*ASL:AMP binary complex formation. ITC data were fitted to one set of site binding model yielding a value of 0.6 (± 0.1) for *n*

(stoichiometry, ligands per active site). This result suggests that more than one subunit of *Lb*ASL contribute to AMP binding. Structural studies showed that three separate protomers contribute to each binding site of tetrameric *M. tuberculosis* ASL[35] and to other enzymes belonging to the Aspartase/Fumarase superfamily.[19] However, the stoichiometry should be equal to approximately one as there are four active sites per tetrameric *Lb*ASL enzyme.

The steady-state kinetic measurements for the reverse reaction and the ITC data for product binding to *Lb*ASL demonstrate that the reaction catalyzed by *Lb*ASL follows an ordered Uni-Bi kinetic mechanism, in which fumarate is the first product to dissociate from the ternary complex followed by AMP release to yield free enzyme for the next round of catalysis (Fig. 7). This proposal is in agreement with *L. donovani* ASL enzyme mechanism.[39]

Energy of activation

The energy of activation (E_a) for the *Lb*ASL-catalyzed chemical reaction was assessed by measuring the dependence of k_{cat} on temperature for S-AMP (Fig. 8). The E_a (6.8 ± 0.3 kcal mol^{-1}) of the reaction was calculated from data fitting to Eq. 8 for the slope ($-E_a/R$) of the Ahrrenius plot (Fig. 8). The transition state enthalpy ($\Delta H^{\#}$ = 6.2 ± 0.3 kcal mol^{-1}), Gibbs free energy ($\Delta G^{\#}$ = 16.4 ± 0.5 kcal mol^{-1}) and entropy ($\Delta S^{\#}$ = -34.4 ± 1.6 cal mol^{-1} K^{-1}) at 25 ºC were calculated using, respectively, Eq. 9, Eq. 10 and Eq. 11. The E_a value of 6.8 kcal mol^{-1} represents the minimum energy needed to initiate the reaction, and the linearity of the Ahrrenius plot suggests that there is no change in the rate-limiting step over the temperature range employed (15 - 40 °C). The $\Delta G^{\#}$ value of 16.4 kcal mol^{-1} represents the energy barrier required for the reaction to occur and can be regarded as the variation of Gibbs energy between the enzyme-substrate activated complex and enzyme-substrate in the ground state.

The negative value for the entropy activation ($\Delta S^{\#}$) suggests that the entropy value for the enzyme:substrate activated complex is lower than the one for enzyme:substrate in the ground state, which may be accounted for by a loss of degrees of freedom on going from the ground state to activated state. The constant A (frequency factor that represents the frequency of collisions between reactant molecules) of Eq. 8 corresponds to the product of collision frequency (Z) and the probability or steric factor (p) from the collision theory of reaction rates. From the absolute rate theory, $A=pZ=(k_BT/h)e^{\Delta S^{\#}/R}$. This equation enables us to interpret the probability factor (p) in terms of the molar entropy of activation

($\Delta S^{\#}$). If reactants are atoms or simple molecules, then relatively little energy is redistributed among the various degrees of freedom in the activated complex (transition-state complex). Consequently, $\Delta S^{\#}$ will be either a small positive or a small negative number, so that $\exp(\Delta S^{\#}/R)$ or *p* is close to unity. But if complex molecules are involved in a reaction, $\Delta S^{\#}$ will be either a large positive or a large negative number. In the former case, the reaction will proceed much faster than predicted by collision theory; in the latter case, a much slower rate will be observed. Note that the probability factor (*p*) takes into account the fact that in a collision complex molecules must be properly oriented to undergo the reaction (having the proper activation energy is a prerequisite but not a guarantee for a reaction to take place). Thus, the frequency factor (A) of the Arrhenius equation depends also on T and *p* (that accounts for that fact that colliding molecules must be properly oriented to undergo the reaction). The negative values for the entropy of activation ($\Delta S^{\#}$) for S-AMP reaction suggests that this reaction proceeds slower than predicted by the collision theory. Incidentally, a value of 17466582 s^{-1} was obtained for A which allows to calculate an apparent first-order constant value of approximately 188 s^{-1} using the Arrhenius equation ($k = Ae^{-Ea/RT}$), which is in reasonably good agreement with the k_{cat} value of 324 s^{-1} from steady-state kinetics data (Table 1).

Solvent kinetic isotope effect (SKIE) and proton inventory

To evaluate the contribution of proton transfer from the solvent to a rate-limiting step of S-AMP conversion into fumarate and AMP for *Lb*ASL, SKIE were determined by data fitting to Eq. 13 (Fig. 9), yielding a value of 1.40 ± 0.06 for ^{D2O}V and of 1.20 ± 0.16 for $^{D2O}V/K$. Isotope effects on *V* report on events following the ternary complex formation capable of undergoing catalysis (fully loaded enzyme), which include the chemical steps, possible enzyme conformational changes, and product release (leading to regeneration of free enzyme). Solvent isotope effects on *V/K* report on the contribution of the proton transfer in steps in the reaction mechanism from binding of the isotopically labeled chemical compound (solvent) to the first irreversible step, usually considered to be the release of the first product (that is, all rate constants from reactant binding until the first irreversible step).[30] As rule of thumb, deuterium accumulates where binding is tighter (that is, fractionation factor is larger than one). Transition state proton contributes the reciprocal of its respective fractionation factor to the solvent isotope effect, whereas the contribution of a reactant state proton to the solvent isotope effect is equal to its fractionation factor.[30]

The values of *V/K* and *V* suggest that there is a modest contribution of solvent proton transference during the rate-limiting step of the reaction, probably events occurring after formation of the binary complex, as conformational and chemical changes. The proton inventory data show that the modest normal SKIE on *V* arises from a single protonic site (Fig. 9 - inset). The SKIE on *V* data are similar to the results observed for *Pf*ASL.[40] On the other hand, there appears to be a modest normal SKIE effect on *V/K* for *Lb*ASL whereas no effect was observed for *Pf*ASL.[40] The latter suggests that subtle differences of substrate binding and solvent proton participation in this process may play a role in *Lb*ASL mode of action. Data fitting to Eq. 14 yielded a transition state fractionation factor ($Ø^T$) value of 0.74, which is in agreement with the value observed for *Pf*ASL enzyme.[40] The transition state fractionation factor value suggests that binding of proton solvent to the transition state and/or to *Lb*ASL en route to catalysis is looser than the S-AMP substrate in the ground state and/or free enzyme as compared to bulk solvent. Solvation catalytic proton bridges are proton transfers that do not have appreciable proton motional amplitude in the reaction coordinate, but occur in stable, normal modes of the transition state.[30] Solvation catalytic proton bridges involve transfers among O, N, and S atoms, for which intrinsic free energy barriers are expected to be small compared to free-energy changes associated with covalent rearrangement of the heavy-atom (nonhydrogenic) framework of the reacting system. Hence, solvation catalytic bridges are strong H bonds with values $Ø^T$ values of 0.3 - 0.6.[30] The $Ø^T$ value thus suggests that solvent proton transfer in transition-state vibrations perpendicular to the reaction coordinate plays a role in *Lb*ASL mode of action. As these proton transfers are common for O and N, it is tempting to suggest that protonation of either His^{197}, His^{119}, Lys^{118}, Gln^{274}, Asn^{330} or Arg^{361} residues, proton transfer from Ser^{322} (or Lys^{118}) to N1/N6 of S-AMP may play a role in *Lb*ALS-catalyzed chemical reaction. However, it should be pointed out that solvent isotope effects lead to isotope exchanges at hundreds of protic positions of the enzyme, which precludes any assignment to a particular chemical group.

pH-rate profiles

In order to gain information on the chemical mechanism of *Lb*ASL and likely residues involved in catalysis and substrate binding, the dependence of kinetic parameters on varying pH values were determined. The pH-rate profile is shown in Fig. 10. The bell-shape pH-rate data for logk_{cat} were fitted to Eq. 15 yielding apparent pK_a value of 7.5 and pK_b value of 9.1, which slopes of +1 for the acidic limb and -1 for the basic limb indicate

the participation of a single ionizable group in each limb. This ionization could be occurring in either the substrate or enzyme.

It is propose that the cleavage of S-AMP to AMP and fumarate for ASL occurs through a general acid-base mechanism involving a β-elimination of fumarate. The reaction initiates by abstraction of the Cβ-proton from the substrate by the general base, resulting in the formation of a carbanion intermediate, and subsequent proton donation by the catalytic acid to the N1 or N6 atom of the substrate results in cleavage of the Cα–N bond and product release.[19,38] The His[197] (for *Lb*ASL counting) is a highly conserved residue in the conserved region C2 in aspartase/fumarase superfamily. This histidine residue has being proposed to act as the general acid, donating a proton to the leaving group.[16,19] In previous site-direct mutagenesis studies, the mutation of correspondent His[171] in *E. coli* ASL,[38] and His[141] in *B. subtilis*,[37] showed decrease in enzyme activity, showing that these histidine residues play a role in catalysis. The His[197] of *Lb*ASL may account for the apparent pK_a value of 7.5 in logk_{cat} analysis, which needs to be deprotonated for catalysis, whereas the pK value from the theoretical histidine imidazole group (pK = 6.0) could be shifted due interactions with others residues in the active site.

Another conserved region in the superfamily is flexible a SS loop which plays an important role in catalysis, performing a conformational change from open to close conformation upon substrate binding in the active site. A lysine residue (Lys[328] *Lb*ASL numbering) situated in the SS loop, has been propose to interact with the α-carboxylate group of the substrate.[19] In addition, this lysine was suggested to be involved in the stabilization of the negative charge of the carbanion intermediate in *E. coli* ASL,[38] *E. coli* L-aspartase[42] and *E. coli* C-fumarase.[43] The apparent pK_b value of 9.1 may correspond to Ser[322] (*Lb*ASL numbering), which could act as the catalytic base. Site-directed mutagenesis studies of the corresponding serines in *B. subtilis* and *H. sapiens* ASL proteins have shown that they are essential for catalysis.[44,45] Nevertheless, site-directed mutagenesis efforts will have to be pursued to ascertain the amino acid residues that play any role in catalysis.

Fitting the data of the rather complex pH-rate profile for k_{cat}/K_M (Fig. 10B) to either Eq. 15 or Eq. 16 yielded poor estimates. For instance, data fitting to Eq. 16 yielded pK values of 6.4 and 9.2 with large errors. The value of 9.2 likely corresponds to the same catalytic group implicated in catalysis by the pH-rate profile for k_{cat} (Fig. 10A). As pH-rate profile studies cannot differentiate between ionizable groups of enzyme and substrate(s). Accordingly, the two ionizing groups in the acidic limb (slope of +2) with a

pK_a value of approximately 6.4 may correspond to either a protein amino acid residue or to the ionization of carboxyl groups of the succinyl moiety of S-AMP substrate whose dissociation constants may have been perturbed by the amino acid side chains of *Lb*ASL.

Conclusion

ASLs have been proposed as potential drug targets due to their important role in purine metabolism.[13,40,46,47] ASL is the last enzyme in the conversion of IMP to AMP. As *Leishmania* species lack the *de novo* pathway and are dependent on the salvage pathway to supply their purine requirements, *Lb*ASL could thus represent a drug target for the development of chemical agents to treat leishmaniasis. As point mutations in the human *purB* ASL-encoding gene causes autosomal recessive disorders such as autism, mental retardation, epilepsy and degeneration of muscles,[48-50] it is of paramount importance that species-specific enzyme inhibitor compounds be designed. Accordingly, exploiting differences in the mode of action between human ASL and enzyme from leishmania represents a promising approach to the design of anti-leishmiasis agents with limited host toxicity. The results presented here may contribute to a better understanding of the biology of *L. braziliensis*, and may aid to the development of *Lb*ASL enzyme inhibitors. Incidentally, it has recently been reported a promising vaccine candidate using a polyvalent α-Gal conjugate on Qβ virus-like nanoparticles that showed elimination of *Leishmania* infection and proliferation of parasites in a C57BL/6 α-galactosyltransferase knockout mouse model.[51] Although these preliminary results bode well, there have to be continuing efforts towards the development of alternatives strategies to combat *Leishmania* infection.

Acknowledgements

This work was supported by funds awarded by Decit/SCTIE/ MSMCT-CNPq-FNDCT-CAPES to National Institute of Science and Technology on Tuberculosis (INCT-TB) to D.S.S. and L.A.B. L.A.B. (CNPq, 520182/99-5), D.S.S. (CNPq, 304051/1975-06), O.N.S. (CNPq, 305984/2012-8), and E.M.C.F. (CNPq, 306706/2014-8) are Research Career Awardees of the National Research Council of Brazil (CNPq). L.G. acknowledges a scholarship awarded by CAPES.

Conflict of interest

The authors declare that they have no conflicts of interest with the contents of this article.

Author contributions

LG, PFD, CDR, ADV and LKBM designed, performed and analyzed all biochemical experiments, and drafted the paper. LFSMT and ONS built the molecular model and interpreted the structure of *Lb*ASL. CVB and ADV designed vectors, and performed cloning and expression. AFPM and CVB designed, performed and analyzed the mass spectrometry experiments. PB, EMCF, DSS and LAB designed experiments and revised critically the manuscript.

References

1. Kaye P., Scott P. Leishmaniasis: complexity at the host–pathogen Interface. *Nat. Rev., Microbiol.,* 2011, **9**, 604-615.

2. WHO. Control of the leishmaniases: report of a meeting of the WHO Expert Committee on the control of Leishmaniases. World Health Organization. Geneva. 2010.

3. Alvar, J. et al. Leishmaniasis worldwide and global estimates of its incidence. *PLoS ONE*, 2012, **7**(5), e35671.

4. Teixeira, D.E. et al. Atlas didático Ciclo de vida da Leishmania.: Fundação CECIERJ, Consórcio CEDERJ, Rio de Janeiro, 2013.

5. Guimarães L.H. et. al. Atypical manifestations of cutaneous Leishmaniasis in a region endemic for *Leishmania braziliensis*: clinical, immunological and parasitological aspects. *PLoS Negl. Trop. Dis.*, 2016, **10**(12):e0005100.

6. Azulay R.D. and Azulay D.R.Jr. Immune-clinical-pathologic spectrum of Leishmaniasis. *International Journal Of Dermatology*, 1995, **34**, 303-307.

7. Croft S.L. and Coombs G.H. Leishmaniasis– current chemotherapy and recent advances in the search for novel drugs. *TRENDS in Parasitology*, 2003, **19**, 502-508.

8. Croft, S. L. and Olliaro, P. Leishmaniasis chemotherapy - challenges and opportunities. *Clin. Microbiol. Infect.*, 2011, **17**, 1478-1483.

9. McGwire, B.S. et. al. Leishmaniasis: clinical syndromes and treatment. *Q. J. Med*, 2014, **107**, 7–14.

10. Lemke, A. et al. Amphotericin B. *Appl. Microbiol. Biotechnol*., 2005, **68**, 151–162.

11. Chawla, B. and Maghubala R. Drug targets in Leishmania. *J. Parasit. Dis*., 2010, **34**(1), 1-13.

12. Marr, J. J. et al. Purine metabolism in *Leishmania donovani* and *Leishmania braziliensis*. *Biochim. Biophys. Acta*, 1978, **544**, 360-371.

13. Boitz, J.M. et al. Adenylosuccinate synthetase and adenylosuccinate lyase deficiencies trigger growth and infectivity deficits in *Leishmania donovani*. *J. Biol. Chem*., 2013, **288**(13), 8977-8990.

14. Boitz, J. M. et al. Purine salvage in Leishmania: complex or simple by design? *TRENDS in Parasitology*, 2012, **28**, 345-352.

15. Berens, R.L. et al. Purine and Pyramidine Metabolism. Biochemistry and Molecular Biology of Parasites. P.89-117. Academic Press Ltd. 1995.

16. Toth, E. A. et al. The structure of adenylosuccinate lyase, an enzyme with dual activity in the *de novo* purine biosynthetic pathway. *Structure*, 2000, **8**, 163-174.

17. Palenchar, J.B., Crocco J.M. and Colman R.F. The characterization of mutant *Bacillus subtilis* adenylosuccinate lyases corresponding to severe human adenylosuccinate lyase deficiencies. *Protein Science*, 2003, **12**, 1694-1705.

18. Ariyananda, L.Z. and Colman, R.F. Evaluation of types of interactions in subunit association in *Bacillus subtilis* adenylosuccinate lyase. *Biochemistry*, 2008, **47**, 2923-2934.

19. Puthan, V.V., Fibriansah, G., Raj, H., Thunnissen, A.W.H. and Poelarends, G.J. Aspartase/Fumarase superfamily: A common catalytic strategy involving general base-catalyzed formation of a highly stabilized *aci*-carboxylate intermediate, *Biochemistry*, 2012, **15**, 15-22.

20. Shevchenko A, Tomas H, Havlis J, Olsen J. V., Mann M. In-gel digestion for mass spectrometric characterization of proteins and proteomes. *Nat. Protoc.*, 2006, **1**(6), 2856-2860.

21. Carvalho, P.C., Lima, D.B., Leprevost, F.V., Santos, M.D., Fischer, J.S., Aquino, P.F. et al., Integrated analysis of shotgun proteomic data with PatternLab for proteomics 4.0, *Nat. Protoc*., 2016, **11**, 102-117.

22. Eng, J.K., Jahan, T.A. and Hoopmann, M.R. Comet: an open source tandem mass spectrometry sequence database search tool. *Proteomics*, 2012, **13**, 22-24.

23. Larkin, M.A., Blackshields, G., Brown, N.P., Chenna, R. P.A. McGettigan, H. McWilliam, F. Valentin, I.M. Wallace, A. Wilm, R. Lopez, J.D. Thompson, T.J. Gibson, D.G. Higgins,Clustal W and Clustal X version 2.0, *Bioinformatics*, 2007, **23**, 2947-2948.

24. Shen M-Y, Sali A. Statistical potential for assessment and prediction of protein structures. Prot Science. 2006; 15:2507–2524.

25. Chen VB, Arendall WB, Headd JJ, Keedy DA, Immormino RM, Kapral GJ, Murray LW, Richardson JS, Richardson DC. MolProbity: all-atom structure validation for macromolecular crystallography. Acta Crystallogr D Biol Crystallogr. 2010b; D66:12–21.

26. Laskowski RA, MacArthur MW, Moss DS, Thornton JM. PROCHECK: a program to check the stereochemical quality of protein structures. J Appl Cryst. 1993; 26:283–291.

27. Segel, I. Enzyme Kinetics, Behavior and Analysis of Rapid Equilibrium and Steady-State Enzyme Systems, John Wiley and Sons, New York, 1975.

28. Lonhienne, T., Baise, E., Feller, G., Bouriotis, V. and Gerday, C. Enzyme activity determination on macromolecular substrates by isothermal titration calorimetry: application to mesophilic and psychrophilic chitinases. *Biochim. Biophys. Acta*, 2001, **1545**, 349-356.

29. Lonhienne, T., Baise, E., Feller, G., Bouriotis, V. and Gerday, C. Psychrophilic enzymes: revisiting the thermodynamic parameters of activation may explain local flexibility. *Biochim. Biophys. Acta*, 2000, **1543**, 1-10.

30. Cook, P.F. Enzyme Mechanism from Isotope Effects, CRC Press, Boca Raton, Florida, 1991.

31. Cook P.F. and Cleland, W.W. Enzyme Kinetics and Mechanism, Garland Science, London and New York, 2007.

32. Lee P. and Colman R. F. Expression, purication, and characterization of stable, recombinant human adenylosuccinate lyase. *Prot. Expr. Pur*., 2007, **51**, 227-234.

33. Lee, T. T., Worby, C., Dixon, J. E. and Coman R. F. Identification of His141 in the active site of *Bacillus subtilis* adenylosuccinate lyase by affinity labeling with 6-(4-Bromo-2,3-dioxobutyl)thioadenisine 5´-Monophosphate. *J. Biol. Chem.*, 1997, **272**, 458-465.

34. Segall M.L., Colman, R.F. Gln212, Asn270, and Arg301 are critical for catalysis by adenylosuccinate lyase from *Bacillus subtilis*. *Biochemistry*, 2004, **43**, 7391-7402.

35. Banerjee S., Agrawal, M.J., Mishra1, D., Sharan, S., Balaram, H., Savithri, H.S. and Murthy M.R.N. Structural and kinetic studies on adenylosuccinate lyase from Mycobacterium *smegmatis* and *Mycobacterium tuberculosis* provide new insights on the catalytic residues of the enzyme. *FEBS Journal*, 2014, **281**, 1642-1658.

36. Bridger, W.A. and Cohen, L.H. The kinetics of adenylosuccinate lyase. *J. Biol. Chem.*, 1968, **243**, 644-650.

37. Lee, T.T., Worby, C., Dixon, J.E., Bao Z., and Colman R.F. His68 and His141 are critical contributors to the intersubunit catalytic site of adenylosuccinate lyase of *Bacillus subtilis*. *Biochemistry*, 1999, **38**, 22-32.

38. Tsai, M., Koo, J., Yip, P., Colman, R.F., Segall, M.L., Howell, P.L. Substrate and product complexes of *Escherichia coli* adenylosuccinate lyase provide new insights into the enzymatic mechanism, *J. Mol. Biol.*, 2007, **370**, 541-554.

39. Spector, T. et al. Specificity of adenylosuccinate synthetase and adenylosuccinate lyase from *Leishmania donovani*. *J. Biol. Chem.*, 1979, **254**, 8422-8426.

40. Bulusu, V. et al. Elucidation of the substrate specificity, kinetic and catalytic mechanism of adenylosuccinate lyase from Plasmodium falciparum. *Biochim. Biophys. Acta*., 2009, **1794**, 642-654.

41. Ladbury J.E. and Doyle, M.L. *Biocalorimetry II*, Wiley, London, 2004.

42. Saribas, S., Schindler, J. F., and Viola R. E. Mutagenic Investigation of Conserved Functional Amino Acids in *Escherichia coli* L-Aspartase. J. Biol. Chem. Vol. 269, No. 9, pp. 6313-6319, 1994.

43. Weaver, T. and Banaszak, L. Crystallographic Studies of the Catalytic and a Second Site in Fumarase C from *Escherichia coli*. Biochemistry 1996, 35, 13955-13965.

44. Sivendran, S. and Colman, R. F. Effect of a new non-cleavable substrate analog on wild-type and serine mutants in the signature sequence of adenylosuccinate lyase of *Bacillus subtilis* and *Homo sapiens*. *Prot. Science* (2008), 17:1162–1174.

45. Segall, M.L., Cashman M. A. and Colman R.F. Important roles of hydroxylic amino acid residues in the function of *Bacillus subtilis* adenylosuccinate lyase. *Prot. Science* (2007), 16:441–448.

46. Spector, T., Berens, R.L., Marr, J.J. Adenylosuccinate synthetase and adenylosuccinate lyase from Trypanosoma cruzi, Specificity studies with potential chemotherapeutic agents, *Biochem. Pharmacol.*, 1982, **31**, 225-229.

47. Fyfe, P.K. et al. Structure of *Staphylococcus aureus* adenylosuccinate lyase (PurB) and assessment of its potential as a target for structure-based inhibitor discovery. *Acta Crystallographica Section D Biological Crystallography.*, 2010, **D66**, 881-888.

48. Jaeken, J., Wadman, S., Duran, M., Van Sprang, F., Beemer, F., Holl, R., Theunissen, P., De Cock, P., Van den Bergh, F. and Vincent, M. Adenylosuccinase deficiency: an inborn error of purine nucleotide synthesis. *Eur. J. Pediatr.*, 1988, **148**, 126-131.

49. Maaswinkel-Mooij, P., Laan, L., Onkenhout, W., Brouwer, O., Jaeken, J. and Poorthuis, B. Adenylosuccinase deficiency presenting with epilepsy in early infancy. *J. Inherit. Metab. Dis.*, 1997, **20**, 606-607.

50. Verginelli, D., Luckow, B., Crifo, C., Salerno, C. and Gross, M. Identification of new mutations in the adenylosuccinate lyase gene associated with impaired enzyme activity in lymphocytes and red blood cells. *Biochim. Biophys. Acta*, 1998, **1406**, 81-84.

51. Moura, A.P.V., Santos, L.C.B., Brito, C.R.N., Valencia, E., Junqueira, C., Filho, A.A.P., Sant'Anna, M.R.V., Gontijo, N.F., Bartholomeu, D.C., Fujiwara, R.T., Gazzinelli, R.T., McKay, C.S., Sanhueza, C.A., Finn, M.G. and Marques, A.F. Virus-like particle display of the α-Gal carbohydrate for vaccination against *Leishmania* infection. *ACS Cent Sci.*, 2017, DOI: 10.1021/acscentsci.7b00311.

52. Robert X and Gouet P. Deciphering key features in protein structures with the new ENDscript server. *Nucleic Acids Res*., 2014, **42**, W320-W324.

53. Sali A, Blundell TL. Comparative protein modelling by satisfaction of spatial restraints. *J. Mol. Biol*., 1993, 234, 779-815.

Figure legends

Figure 1: Multiple sequence alignment of ASL from *Leishmania braziliensis* (*Lb*ASL, XP_001561734), *Leishmania donovani* (*Ld*ASL, XP_003858107), *Escherichia coli* (*Ec*ASL, WP_000423742), *Plasmodium falciparum* (*Pf*ASL, XP_001349577), *Bacillus subtilis* (*Bs*ASL, WP_003233955), *Homo sapiens* (*Hs*ASL, NP_000017), *and Mycobacterium tuberculosis* (*Mt*ASL, WP_003898583). Residues His119, His197, S322, and K328, proposed to be involved in catalysis, are indicated by black solid circles. ASL enzymes present three highly conserved regions, C1, C2, and C3 (residues 147 - 158, 194 - 204, and 321 - 331 in *Lb*ASL), which in the structure pack together to form the active site. The red boxes represent residues conserved in all sequences. The yellow box represents residues that present the same physical-chemical properties. The alignment was prepared with ClustalW[52] and ESPript.[53]

Figure 2: Structure organization of the ASL from *Leishmania braziliensis* (*Lb*ASL). *Lb*ASL is biologically active as a homotetramer and contains four active sites. Amino acid resudies of three subunits contribute to each enzyme active. (A) Quaternary structure of *L*bASL and a close view of the active site, which is formed by tight packing of regions C1 (red), C2 (blue), and C3 (green), belonging to, respectively, monomers D, A, and B. (B) Representation of the N-terminal (D1), central core (D2) and C-terminal (D3) domains of one enzyme subunit. Protein main polypeptide chain, represented as cartoon, is coloured in grey, and AMP and fumarate are represented as sticks and coloured as CPK. The illustration was generated with PyMOL (The PyMOL Molecular Graphics System, Version 1.8 Schrödinger, LLC).

Figure 3: The proposed residues involved in the reaction mechanism. This model of *Lb*ASL active site shows contacts of the imidazole side chain of His^{197} with AMP, and the putative catalytic base Ser^{322} with the C(β or α)-H of the succinyl moiety of the substrate. Protein main-chain, represented as cartoon, is coloured in grey, and AMP, fumarate and amino acid residues are represented as sticks and coloured as CPK. The illustration was generated with PyMOL (The PyMOL Molecular Graphics System, Version 1.8 Schrödinger, LLC).

Figure 4: Initial velocities for S-AMP conversion into AMP and fumarate. Substrate saturation curve was hyperbolic and data fitted to Eq. 2.

Figure 5: Intersecting initial velocity patterns for ASL using either fumarate (a) or AMP (b) as the variable substrate. Each curve represents varied-fixed levels of the substrate.

Figure 6: ITC analysis of *Lb*ASL titration with AMP. The top panels show raw data of the heat pulses resulting from titration of *Lb*ASL. The botton panels show the integrated heat pulses, normalized per mole of injection as a function of the molar ratio (ligand concentration/*Lb*ASL subunit concentration). Data were best fitted to a one binding site model.

Figure 7: Proposed sequential ordered Uni-Bi kinetic mechanism for *Lb*ASL, in which fumarate release is followed by AMP dissociation to form free enzyme.

Figure 8: Temperature dependence of ln k_{cat}. Saturating concentrations of S-AMP substrate were employed to measure the maximum velocity as a function of temperature ranging from 15 to 40 °C. The linearity of the Arrhenius plot suggests that there is no change in the rate-limiting step over the temperature range utilized in this assay.

Figure 9: Solvent kinetic isotope effects for *Lb*ASL. S-AMP was used as the variable substrate (5-100 μM). Reaction mixtures contained either 0 (♦) or 90 (●) atom % D_2O. The inset represents the proton inventory (0, 20, 40, 60 and 90 atom % D_2O) measuring *Lb*ASL enzyme activity at fixed-saturating concentration of S-AMP (100 μM), in which the y-axis represents the values for k_{cat} in solutions containing different mole fractions of D_2O (k_n) divided by k_{cat} in H_2O (k_0), and the x-axis gives the isotopic composition of the solvent (n).

Figure 10: Dependence of steady-state kinetic parameters on different pH values for *Lb*ASL reaction. (A) Data for pH dependence of log k_{cat} were fitted to Eq 15. (B) Data for the dependence of log k_{cat}/K_M on pH values were fitted to Eq. 16.

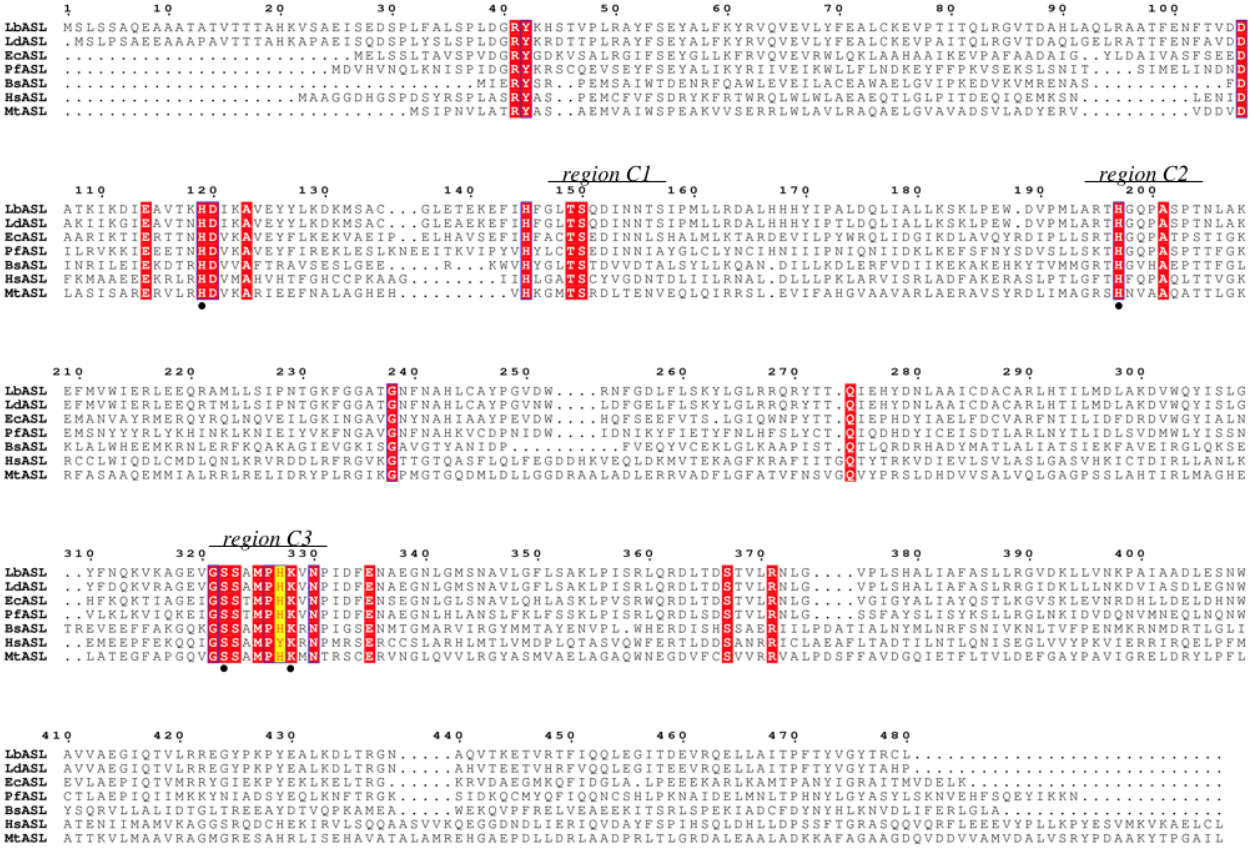
region C1
region C2
region C3
LbASL
LdASL
EcASL
PfASL
BsASL
HsASL
MtASL

FIGURE 1

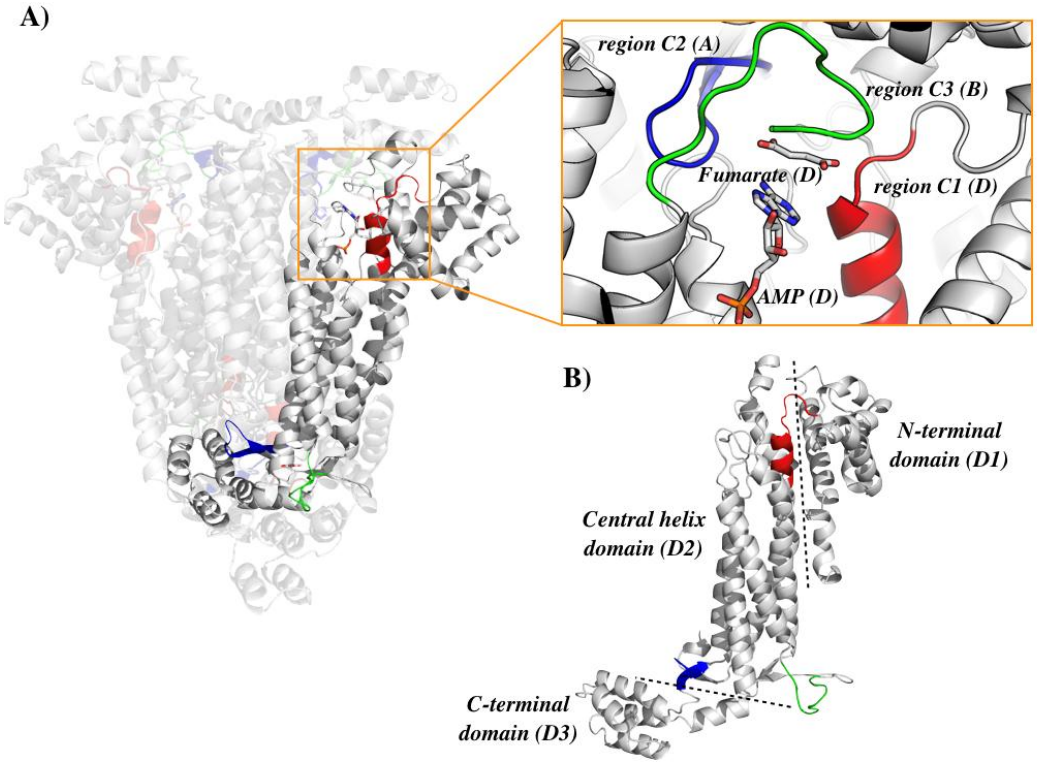
A)
region C2 (A)
region C3 (B)
Fumarate (D)
region C1 (D)
AMP (D)
B)
N-terminal
domain (D1)
Central helix
domain (D2)
C-terminal
domain (D3)

FIGURE 2

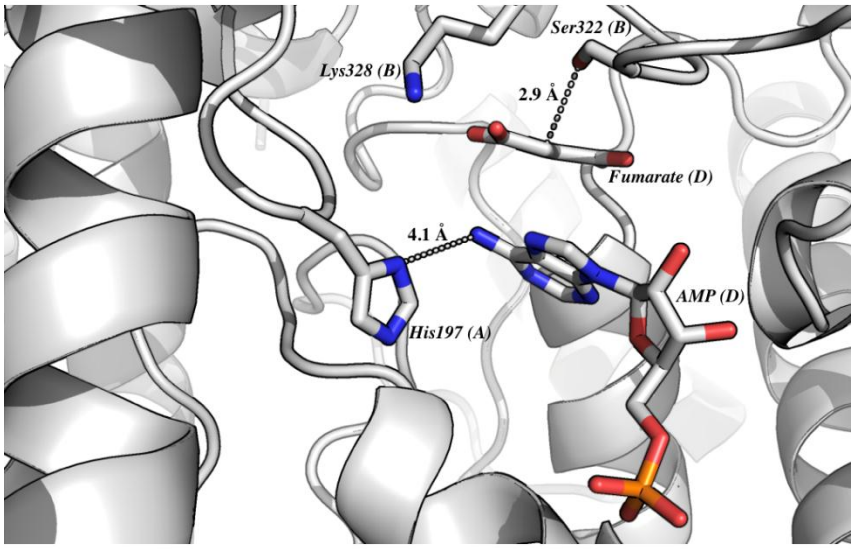

FIGURE 3

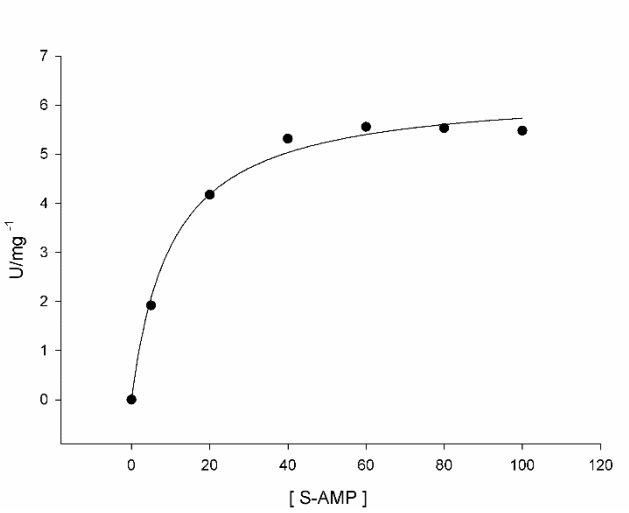

FIGURE 4

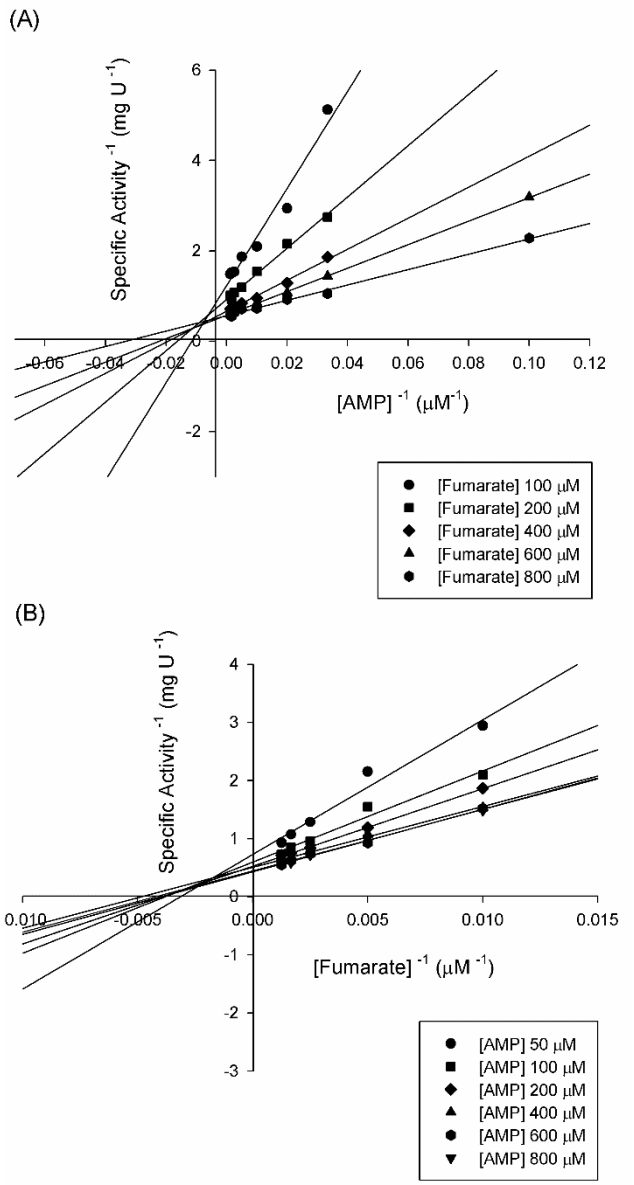
(A)
Specific Activity -1 (mg U -1)
6
4
2
0
-2
-0.06
-0.04
-0.02
0.00
0.02
0.04
0.06
0.08
0.10
0.12
[AMP] -1 (μM-1)
[Fumarate] 100 μM
[Fumarate] 200 μM
[Fumarate] 400 μM
[Fumarate] 600 μM
[Fumarate] 800 μM
(B)
Specific Activity -1 (mg U -1)
4
3
2
1
0
-1
-2
-3
0.010
-0.005
0.000
0.005
0.010
0.015
[Fumarate] -1 (μM -1)
[AMP] 50 μM
[AMP] 100 μM
[AMP] 200 μM
[AMP] 400 μM
[AMP] 600 μM
[AMP] 800 μM

FIGURE 5

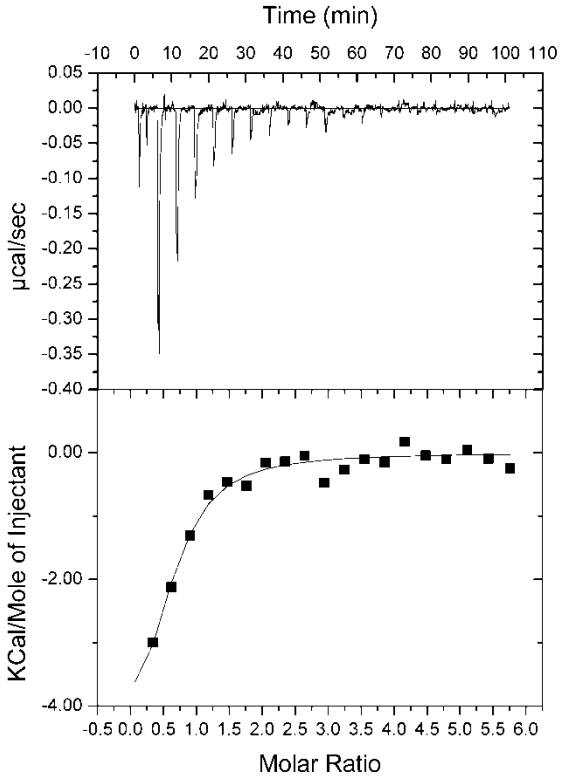
Time (min)
-10 0 10 20 30 40 50 60 70 80 90 100 110
0.05
0.00
-0.05
-0.10
-0.15
-0.20
-0.25
-0.30
-0.35
-0.40
µcal/sec
0.00
-2.00
-4.00
KCal/Mole of Injectant
-0.5 0.0 0.5 1.0 1.5 2.0 2.5 3.0 3.5 4.0 4.5 5.0 5.5 6.0
Molar Ratio

FIGURE 6

FIGURE 7

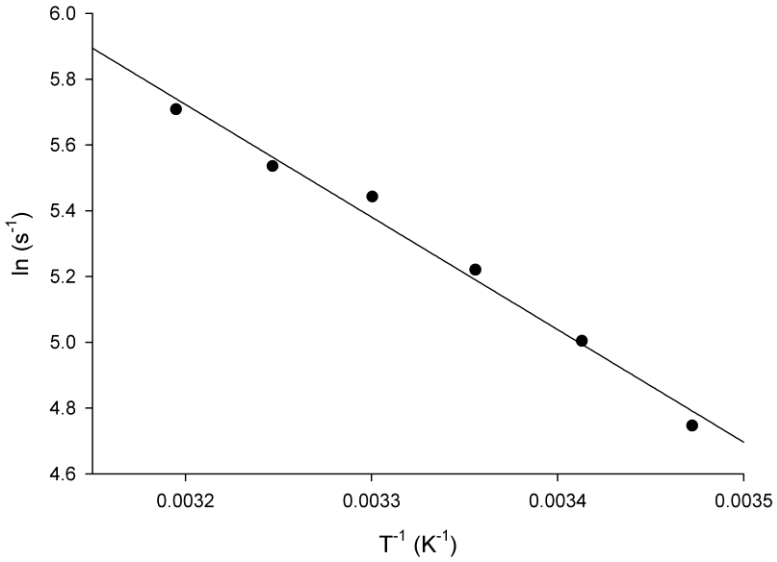

FIGURE 8

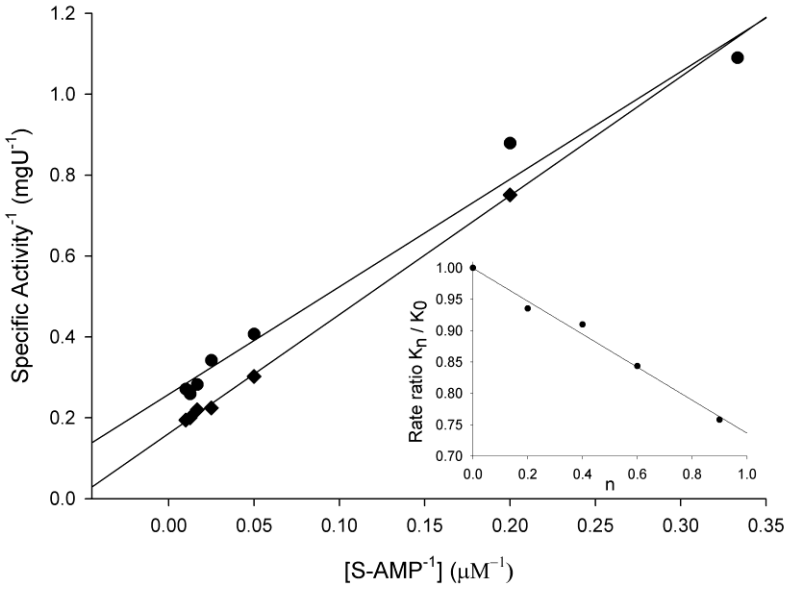

FIGURE 9

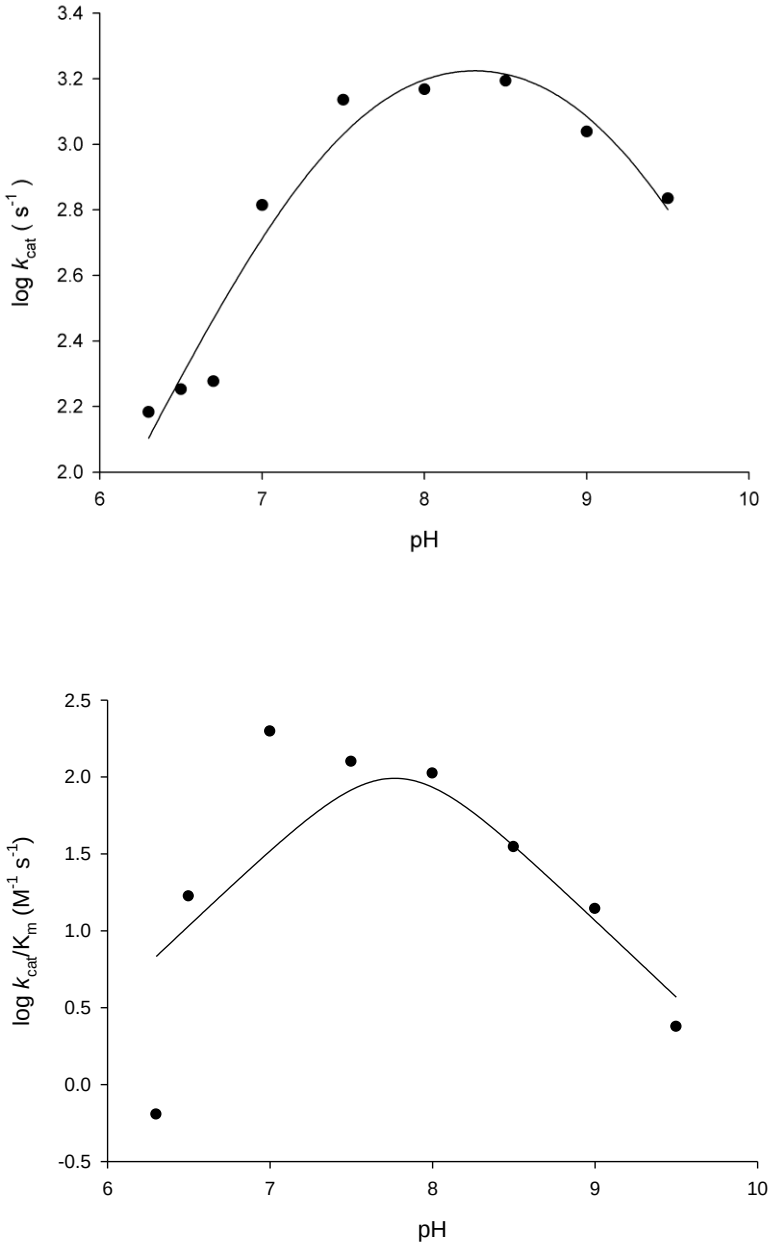
3.4
3.2
3.0
2.8
2.6
2.4
2.2
2.0
log k_{cat} (s^{-1})
6
7
8
9
10
pH
2.5
2.0
1.5
1.0
0.5
0.0
-0.5
log k_{cat}/K_m (M^{-1} s^{-1})
6
7
8
9
10
pH

FIGURE 10

Capítulo 3

Considerações finais

Perspectivas

4. CONSIDERAÇÕES FINAIS

A leishmaniose é uma doença infecciosa, não contagiosa causada por protozoários do gênero *Leishmania*, sendo considerada um importante problema de saúde pública mundial. Em humanos, a infecção por *Leishmania* pode causar lesões que comprometem a pele, as mucosas das vias respiratórias superiores e as vísceras. O tratamento padrão disponível utiliza de medicamentos que apresentam efeitos colaterais severos e precisam ser administrados em âmbito hospitalar, o que dificulta a aderência do paciente pelo tratamento. Neste contexto, o desenvolvimento de fármacos eficazes, menos tóxico e de fácil administração se faz necessário para redução da incidência das leishmanioses.

Devido à importância da via de salvamento de purinas para o parasita, as enzimas envolvidas nesta via podem ser possíveis alvos moleculares interessantes na busca de compostos inibidores, uma vez que essa é a única forma das leishmanias adquirirem os nucleotídeos purínicos, visto que a via de biossíntese *de novo* está ausente nesses organismos. A enzima ASL é a última enzima responsável pela conversão de IMP a AMP em *Leishmania*, representando dessa forma um passo crucial para síntese de purinas, o que a torna um alvo atrativo para o desenvolvimento de novos fármacos.

Este trabalho apresenta os resultados da clonagem do gene ASL de *Leishmania braziliesis*, da expressão da proteína recombinante e da obtenção da proteína em sua forma homogênea a partir de um protocolo de purificação que consiste de duas colunas cromatográficas. A partir do sequenciamento peptídico, foi confirmada a identidade da proteína recombinante. A determinação do estado oligomérico sugere que a *Lb*ASL é um tetrâmero em solução. O alinhamento múltiplo de sequências de aminoácidos permitiu propor os prováveis resíduos de aminoácidos envolvidos na catálise e na ligação com o substrato. Os resultados obtidos de cinética em estado estacionário mostraram que a enzima segue o perfil de Michaelis-Menten. A determinação das velocidades iniciais da reação reversa apresentou uma família de linhas que se intersectam a esquerda do eixo y, sugerindo a formação de um complexo ternário e um mecanismo sequencial para a reação reversa. A determinação da constante de equilíbrio (K_{eq} = 6280 µM) sugere que a reação direta catalisada pela *Lb*ASL não é favorável sob as condições empregadas *in vitro*.

Estudos de calorimetria de titulação isotérmica (ITC) também foram realizados, os resultados sugerem que a reação catalisada pela *Lb*ASL segue um mecanismo cinético Uni-Bi ordenado, no qual o fumarato é o primeiro produto a deixar o sítio ativo da enzima seguido pelo AMP. O valor negativo obtido para a entalpia indica uma pequena, mas favorável redistribuição de interações interatômicas (ligações de hidrogénio e/ou van der Waals) e a liberação de moléculas de água do sítio ativo da enzima entre as espécies reativas, incluindo o solvente. O valor positivo obtido para entropia sugere tanto a liberação de moléculas de água e/ou uma mudança no estado conformacional da *Lb*ASL ou do AMP na formação do complexo binário. O valor negativo para a energia livre de Gibbs sugere um processo favorável para a formação do complexo binário *Lb*ASL:AMP. O valor obtido para estequiometria sugere que mais de uma subunidade da proteína está envolvida no sítio de ligação do AMP. Os parâmetros termodinâmicos de ativação para a reação catalisada pela *Lb*ASL foram determinados por meio do ensaio de energia de ativação com o substrato S-AMP. O valor de E_a = 6,8 kcal mol^{-1} representa a energia mínima necessária para iniciar a reação e a linearidade do gráfico utilizando a equação de Ahrrenius sugere que não há mudanças de temperatura na etapa limitante da reação. Outros parâmetros termodinâmicos de ativação ($\Delta G^{\#}$, $\Delta S^{\#}$, $\Delta H^{\#}$) também foram obtidos.

Estudos relacionados ao efeito isotópico do solvente em *V* indicam um efeito de transferência de prótons nos eventos que seguem a formação do complexo ternário capaz de sofrer catálise, os quais incluem as etapas químicas, as mudanças conformacionais da enzima e a liberação dos produtos. Efeitos isotópicos em *V/K* sugerem uma contribuição da transferência de prótons no mecanismo de reação da ligação do solvente no primeiro passo irreversível, usualmente considerado ser a liberação do primeiro produto. O inventário de prótons mostra que o efeito isotópico em *V* surge a partir de um único próton.

O ensaio de perfil de pH para k_{cat} gerou os valores de p*Ks* de 7,5 e 9,1 indicando que há a participação de dois grupos ionizáveis durante a catálise. A análise dos resultados obtidos no ensaio de perfil de pH, juntamente com os dados do alinhamento da sequência de aminoácidos e da modelagem molecular da *Lb*ASL possibilitou sugerir que os resíduos de aminoácidos His^{197} e Ser^{322} estejam envolvidos na catálise. A análise dos dados do perfil de pH para k_{cat}/K_M

foi mais complexa, gerando valores de p*K*s de 6,4 e 9,2 com erros elevados. O valor de 9,2 provavelmente corresponde ao mesmo grupo catalítico indicado na análise de perfil de pH para k_{cat}. O valor de p*K* de 6,4 pode corresponder tanto aos resíduos de aminoácidos quanto a ionização dos grupos carboxílicos da porção succinil do substrato, cujas constantes de dissociação podem ter sido perturbadas pelas cadeias laterais de aminoácidos de *Lb*ASL.

Os objetivos propostos no trabalho, com exceção da obtenção da estrutura cristalográfica, foram realizados com sucesso. Estes resultados possibilitaram a caracterização bioquímica e estrutural da enzima *Lb*ASL, no entanto, estudos adicionais ainda são necessários para a melhor compreensão do mecanismo de ação da enzima. A resolução da estrutura cristalográfica possibilitará identificar as interações entre os grupamentos funcionais das cadeias laterais dos resíduos de aminoácidos no sítio ativo da enzima com os substratos e/ou inibidores. Experimentos de mutagênese sítio-direcionadas são necessários para melhor identificação e compreensão do papel de resíduos de aminoácidos importantes para a catálise da ASL.

REFERÊNCIAS

1 – Manual de Controle da Leishmaniose Tegumentar Americana. FUNASA: 62 p. 2000.

2 – WHO. Control of the leishmaniases: report of a meeting of the WHO Expert Committee on the Control of Leishmaniases. World Health Organization. Geneva. 2010.

3 – Organización Panamericana de la Salud. Leishmaniasis En Las Américas Recomendaciones Para El Tratamiento. Washington, DC, 2013.

4 – Teixeira, D. E. et al. Atlas didático Ciclo de vida da *Leishmania*.: Fundação CECIERJ, Consórcio CEDERJ, Rio de Janeiro, 2013.

5 – Kaye P., Scott P. Leishmaniasis: complexity at the host–pathogen Interface. Nature Reviews, Microbiology. V.9, p.604-615. August, 2011.

6 – Manual de Vigilância da Leishmaniose Tegumentar Americana. EPIDEMIOLÓGICA, D. D. V. 2010.

7 – Dantas, M. L. Aspectos Comparativos Da Resposta Inflamatória Em Lesões De Leishmaniose Cutânea Localizada e Disseminada. 94 Centro De Pesquisas Gonçalo Moniz, Fundação Oswaldo Cruz, Salvador. 2012.

8 – David, C. V. and Craft, N. Cutaneous and mucocutaneous leishmaniasis Dermatologic Therapy, Vol. 22, 491–502. 2009.

9 – Manual de Zoonoses. V.1 2ª Edição 2010.

10 – Alvar, J. et al. Leishmaniasis Worldwide and Global Estimates of Its Incidence. PLoS ONE 7(5): e35671. May, 2012.

11 – Karagiannis-Voules, D. A. et al. Bayesian Geostatistical Modeling of Leishmaniasis Incidence in Brazil. PLoS Negl Trop Dis 7(5): e2213. 2013.

12 – Portal da saúde, Ministério da Saúde. http://portalsaude.saude.gov.br/images/pdf/2016/novembro/08/LV-Casos.pdf e http://portalarquivos.saude.gov.br/images/pdf/2017/setembro/14/LT-Casos.pdf.

13 – Gontijo, B., Carvalho, M. L. R. Leishmaniose tegumentar americana. Revista da Sociedade Brasileira de Medicina Tropical 36(1):71-80, jan-fev, 2003.

14 – Handman, E. and Bullen, D. V. R. Interaction of *Leishmania* with the host macrophage. TRENDS in Parasitology Vol.18 No.8, August, 2002.

15 – Moal, V. L. and Loiseau, P. M. *Leishmania* hijacking of the macrophage intracelular compartments. FEBS Journal 283. P. 598–607, 2015.

16 – Rittig, M.G. and Bogdan, C. Leishmania–Host-cell Interaction: Complexities and Alternative Views. Parasitology Today, vol. 16, no. 7, 2000.

17 – Belaz, S. et al. Identification, biochemical characterization, and *in-vivo* expression of the intracellular invertase BfrA from the pathogenic parasite *Leishmania major*. Carbohydrate Research 415. P. 31–38. 2015.

18 – Peters, N. C. et al. In vivo imaging reveals an essential role for neutrophils in Leishmaniasis transmitted by sand flies. Science. 15; 321(5891): 970–974. August, 2008.

19 – Lacerda, A. F. et al. Anti-parasitic Peptides from Arthropods and their Application in Drug Therapy. Frontiers in Microbiology. V. 7. Article 91. February, 2016.

20 – McGwire, B.S. et. al. Leishmaniasis: clinical syndromes and treatment. Q J Med; 107:7–14. 2014.

21 – Haldar, A. K. et al. Use of Antimony in the Treatment of Leishmaniasis: Current Status and Future Directions. Molecular Biology International. Volume 2011, Article ID 571242, 23 pages. doi:10.4061/2011/571242. 2011.

22 – Sundar, S. et al. Comparison of short-course multidrug treatment with standard therapy for visceral leishmaniasis in India:an open-label, non-inferiority, randomised controlled trial. www.thelancet.com. Vol 377, February 5, 2011.

23 – Lemke, A. et al. Amphotericin B. Appl Microbiol Biotechnol. 68: 151–162, 2005.

24 – Sundar, S. et al. Visceral leishmaniasis - current therapeutic modalities. Indian J. Med. Res. 123, pp 345-352. March, 2006.

25 – Almeida, R. et al. Randomized, Double-Blind Study of Stibogluconate Plus Human Granulocyte Macrophage Colony-Stimulating Factor versus Stibogluconate Alone in the Treatment of Cutaneous Leishmaniasis. The Journal of Infectious Diseases 1999;180:1735–7.

26 – Santos, J. B. et al. Antimony plus Recombinant Human Granulocyte-Macrophage Colony-Stimulating Factor Applied Topically in Low Doses Enhances Healing of Cutaneous Leishmaniasis Ulcers: A Randomized, Double-Blind, Placebo-Controlled Study. The Journal of Infectious Diseases 2004; 190:1793–6.

27 – Prasad, N. et al. Heat, Oriental sore, and HIV. www.thelancet.com Vol. 377, February 12, 2011.

28 – Moura, A.P.V., Santos, L.C.B., Brito, C.R.N., Valencia, E., Junqueira, C., Filho, A.A.P., Sant'Anna, M.R.V., Gontijo, N.F., Bartholomeu, D.C., Fujiwara, R.T., Gazzinelli, R.T., McKay, C.S., Sanhueza, C.A., Finn, M.G. and Marques, A.F. Virus-like particle display of the α-Gal carbohydrate for vaccination against Leishmania infection. ACS Cent Sci., 2017, DOI: 10.1021/acscentsci.7b00311.

29 – Hassan, H. F. and Coombs, G. H. A Comparative Study Of The Purine- And Pyrimidine-Metabolising Enzymes Of A Range Of Trypanosomatids. Comp. Biochem. Physiol. Vol. 84B, No. 2, pp. 217-223, 1986.

30 – Kouni, M. H. Potential chemotherapeutic targets in the purine metabolism of parasites. Pharmacology & Therapeutics 99, 283– 309. 2003.

31 – Cushnan, D.W. et al. Rational Desing and Biochemical Utility of Specific Inhibitor of Angiotensin-Converting Enzyme. Journal of Cardiovascular Pharmacology. 10 (Suppl. 7):S17-S30. New York. 1987.

32 – Berens, R.L. et al. Purine and Pyramidine Metabolism. Biochemistry and Molecular Biology of Parasites. P.89-117. Academic Press Ltda. 1995.

33 – Hammond, D. J. et al. Purine And Pyrimidine Metabolism In The Trypanosomatidae. Molecular and Biochemical Parasitology, 13, 243-261. 1984.

34 – Marr, J. J. et al. Purine Metabolism In Leishmania Donovani And *Leishmania braziliensis*. Biochimica et Biophysica Acta, 544, 360—371. 1978.

35 – Nelson, L. D. and Cox, M. M. Princípios de Bioquímica de Lehninger – Cap. 22, p. 910. 6ª Ed. Omega. 2014

36 – Voet, D. and Voet, J. G. Bioquímica. Cap. 28, p. 1113-1120. 3ª Ed. Panamericana. 2006.

37 – Stryer, L. Biohemistry. Cp. 25, p. 495-501. 4ª Ed. Guanabara Koogan S.A. 1992.

38 – Vierira, E. C. et al. Biologia celular e biologia molecular. Cap. 16, p 261-270. 2ª Ed. Atheneu. 1999.

39 – Boitz, J. M. et al. Purine salvage in *Leishmania*: complex or simple by design? Trends in Parasitology, Vol. 28, No. 8. August ,2012.

40 – Ducati, R.G. et al. Purine Salvage Pathway in *Mycobacterium tuberculosis.* Current Medicinal Chemistry, 18, 1258-1275. 2011.

41 – Carter NS, Yates P, Arendt CS, Boitz JM, Ullman B. Purine and pyrimidine metabolism in *Leishmania*. Adv Exp Med Biol. 2008; 625:141-54.

42 – Boitz, J. M. et al. Adenylosuccinate Synthetase and Adenylosuccinate Lyase Deficiencies Trigger Growth and Infectivity Deficits in *Leishmania donovani*. J. Biol. Chem. Mar 29; 288(13): 8977–8990, 2013.

43 – Boitz JM, Jardim A, Ullman B. GMP reductase and genetic uncoupling of adenylate and guanylate metabolism in Leishmania donovani parasites. Molecular and Biochemical Parasitology http://dx.doi.org/10.1016/j.molbiopara.2016.06.008.

44 – Spector, T. et al. Specificity of Adenylosuccinate Synthetase and Adenylosuccinate Lyase from Leishmania donovani. The .Journal Of Biological Chemistry Vol. 254. No. 17, I.ssue of September 10, pp. 8422-8426. 1979.

45 – Banerjee, S. et al. Structural and kinetic studies on adenylosuccinate lyase from *Mycobacterium smegmatis* and *Mycobacterium tuberculosis* provide new insights on the catalytic residues of the enzyme. FEBS Journal 281, 1642–1658, 2014.

46 – Lee, T. T. et al. Identification of His141 in the Active Site of *Bacillus subtilis* Adenylosuccinate Lyase by Affinity Labeling with 6-(4-Bromo-2,3-dioxobutyl)thioadenosine 5*-Monophosphate. The Journal Of Biological Chemistry. Vol. 272, No. 1, Issue of January 3, pp. 458–465, 1997.

47 – Bridger, W. A. et al. The Kinetics of Adenylosuccinate Lyase. The Journal Of Boilocical Chemistry. Vol. 243, No. 3, Issue of February 10, pp. 644-650, 1968.

48 – Ariyananda, L. Z. et al. In vitro Hydridization and Separation of Hybrids of Human Adenylosuccinato Lyase from Wild-Type and Disease-Associated Mutant Enzymes. Biochemistry. Vol.50:1336-1346. 2011

49 – Palenchar, B.J. et al. Characterization of a Mutant *Bacillus subtilis* Adenylosuccinate Lyase to a Mutant Enzyme Found in Human Adenylosiccinate Lyase Deficiency: Asparagine 276 Plays an Important Structural Role. Biochemistry. Vol.42:1831-1841. 2003

50 – Toth, E. A. et al. The Crystal Structure of Adenylosuccinate Lyase from *Pyrobacculum aerophilum* revels an Intracellular Protein with Tree Disulfite Bonds. J. Bio. Mol. Vol.31:433-450. 2000

51 – Toth, E. A. et al. The structure of adenylosuccinate lyase, an enzyme with dual activity in the *de novo* purine biosynthetic pathway. Structure, Vol. 8, No.2. 2000.

52 – Buluso, V. et al. Elucidaion of the substrate specificity, kinetic and catalytic mechanism of adenylosuccinate lyase from *Plasmodium falciparum*. Biochimica at Biophysica Acta. Vol.1794. p. 642-654. 2009.

53 – Ducati, R. G. et al. Transition-state inhibitors of purine salvage and other prospective enzyme targets in malaria. National Institutes of Health 5(11). 2013.

54 – Fyfe,P. K. et al. Structure of *Staphylococcus aureus* adenylosuccinate lyase (*PurB*) and assessment of its potential as a target for structure-based inhibitor discovery. Acta Crystallographica Section D Biological Crystallography. D66, 881–888. 2010.

55 – Carvalho, P. C. et al. Integrated analysis of shotgun proteomic data with PatternLab for proteomics 4.0. Nature Protocols 11, 102–117. 2016.